UMEÅ UNIVERSITY

LRIG1 in lung cancer

Prognostic effects and mechanistic studies

Samuel Kvarnbrink

Department of Radiation Sciences
Umeå 2020

This work is protected by the Swedish Copyright Legislation (Act 1960:729)
Dissertation for PhD

ISBN: 978-91-7855-412-6 (print)
ISBN: 978-91-7855-413-3 (pdf)
ISSN: 0346-6612
New series number 2108

Cover: Lungworts, *Pulmonaria* spp., were believed to relieve respiratory ailments. Watercolor on paper. Artist Britt-Marie Eliasson, used with permission.

Electronic version available at: http://umu.diva-portal.org/
Printed by: CityPrint i Norr AB
Umeå, Sweden 2020

Choose my aim, take one step and then the next.
It had never been anything else.

— Ann Leckie, *Ancillary Justice*

Table of contents

Abstract iii

Original papers v

Co-authored original papers not included in thesis. vi

Abbreviations. vii

Populärvetenskaplig sammanfattning på svenska. ix

Introduction 1

Treatment by clinical stage 2

Localized disease — stage I and II *3*

Locally advanced disease — stage III *4*

Metastatic disease — stage IV *5*

Medical treatment 6

Chemotherapy. *6*

Tyrosine kinase inhibitors *6*

Immunotherapy *7*

Prognostic factors 9

Molecular prognostic markers. *9*

Predictive markers for chemotherapy. 10

Predictive markers for targeted therapies 13

EGFR. *13*

ALK and ROS1 . . . . . *15*

MET *16*

BRAF *17*

Predictive markers for immunotherapy. 17

LRIG proteins 18

LRIG proteins in non-small cell lung cancer *21*

Aims 22

Materials and methods 23

Tissue microarray and immunohistochemical staining. 23

In silico and quantitative RT-PCR gene expression analyses . . . 25
Statistical methods and survival analysis . . . 26
Generation of plasmids and lentiviral particles . . . 27
Cell culture and reagents . . . 29
Lentiviral transductions and transient transfections . . . 29
Yeast two-hybrid screening . . . 30
Western blotting and co-immunoprecipitation . . . 31
Immunofluorescence and co-localization assays . . . 32
Proximity ligation assay . . . 33
Animal strains and husbandry . . . 33
Ethical considerations . . . 34
Orthotopic implantation . . . 34
Magnetic resonance imaging . . . 35
Digital droplet PCR . . . 35
Transwell and wound closure assays . . . 36
Live-cell imaging assays . . . 37
Radiosensitivity and clonogenicity assays . . . 37
Dose response and cell proliferation assays . . . 38
Results and discussion . . . 39
LRIG1 was a positive prognostic marker for survival in early-stage NSCLC (I) . . . 39
LRIG1 and LRIG3 interacted physically with LMO7 and LIMCH1 (II) . . . 40
LMO7 and *LIMCH1* were downregulated in NSCLC and the prognostic value of LRIG1 expression was dependent on LMO7 status (II) . . . 44
LRIG1 overexpression did not affect cell proliferation in most cell lines (III) . . . 46
LRIG1 overexpression had inconsistent effects on migration but affected clonogenic ability (III) . . . 47
Chemo- and radiosensitivity was unaffected by LRIG1 overexpression (III) . . . 48
LRIG1 was not significantly enriched in metastases compared to primary tumors (III) . . . 49
Conclusions . . . 51
Acknowledgements . . . 52
References . . . 54

Abstract

Lung cancer is the leading cause of cancer-related death worldwide as well as in Sweden. Non-small cell lung cancer (NSCLC) is the predominant form, which is largely subdivided into adenocarcinomas and squamous cell carcinomas. A small minority of NSCLC cases that present with localized small tumors are curable with surgery alone, but adjuvant chemotherapy is recommended in most cases that are treated with surgery, even though it only increases the chance of cure by less than 5%. Therefore, additional biomarkers are needed to guide the clinical decision making in early-stage disease.

The leucine-rich repeats and immunoglobulin-like (LRIG) family of proteins consists of three paralogous transmembrane proteins that are involved in the regulation of growth factor signaling. Of these proteins, LRIG1 is the most studied and it interacts with a wide variety of growth factor receptors and related proteins, including the epidermal growth factor (EGFR) and several others. High levels of LRIG1 have been associated with better survival in a multitude of malignant diseases, including (but not limited to) breast cancer, bladder cancer, cervical cancer, glioma and melanoma. The aim of this thesis was to investigate whether LRIG1 was a prognostic factor in NSCLC as well, and to further characterize the biological role of LRIG proteins in this disease.

To investigate the prognostic impact of LRIG proteins in NSCLC, we stained a tissue microarray (TMA) containing tumor samples from 347 surgically treated early-stage NSCLC patients for LRIG1, LRIG2 and LRIG3. LRIG1 high-expressing adenocarcinoma cases had a large and statistically significant survival benefit of 33 months compared to negative cases. Similarly, an *in silico* analysis of a large gene expression dataset from the Oncomine database showed that high *LRIG1* mRNA expression was linked to better survival as well. Differences in survival persisted even when adjusting for known prognostic factors, meaning that LRIG1 was an independent positive prognostic marker for survival in NSCLC.

A yeast two-hybrid screen was performed to search for proteins interacting with a conserved cytosolic peptide shared between all three mammalian LRIG proteins. This screen yielded hits for the paralogous proteins LIM domain only protein 7 (LMO7) and LIM and calponin homology domains-containing protein 1 (LIMCH1). LRIG1 and LRIG3 were both found to physically interact with LMO7 and LIMCH1 as assessed through immunoprecipitation techniques on overexpressed proteins. For LMO7, this could also be confirmed at endogenous

protein levels using the proximity ligation assay. The 347 samples in the previously mentioned TMA were stained for LMO7. In our survival analysis, we observed no significant survival differences when looking at LMO7 alone, but the survival benefit observed for high LRIG1 was found to be limited to the subgroup that also was negative for LMO7. This means that the observed physical interaction between LRIG1 and LMO7 appears to translate to differences in patient survival.

To investigate possible mechanisms underlying the observed association between high LRIG1 expression and a favorable patient survival, a panel of NSCLC cell lines was modified to overexpress LRIG1. Broadly, LRIG1 overexpression resulted in minor decreases in cellular proliferation rates and no effects on chemosensitivity or radiosensitivity. Looking across the panel of NSCLC cell lines, no clear pattern was observed regarding the effects of LRIG1 overexpression on cellular motility. However, LRIG1 overexpression significantly decreased the clonogenic potential in most cell lines. The only cell line in the panel, H1299, that formed hematogenous disseminated disease in immunodeficient mice was used to establish a mixed-population primary tumor of tagged LRIG1 overexpressing cells and control cells. The LRIG1 transduced cells were was found to be enriched in the injected primary tumor, but no significant changes in their relative abundance was observed between the metastatic sites and their corresponding primary tumors.

In summary, we found that LRIG1 was an independent positive prognostic factor in early-stage NSCLC. We identified LMO7 and LIMCH1 as interaction partners for LRIG proteins and showed that the interaction between LMO7 and LRIG1 had implications for the clinical outcome in NSCLC. Furthermore, our mechanistic studies on the effects of LRIG1 overexpression on NSCLC cells suggested that the survival benefit conferred by high LRIG1 expression may be due to differences in metastatic potential. Taken together, the findings in this thesis suggest an important biological role for LRIG proteins in NSCLC.

Original papers

Paper I **Kvarnbrink S**, Karlsson T, Edlund K, Botling J, Lindquist D, Jirström K, Micke P, Henriksson R, Johansson M, Hedman H. LRIG1 is a prognostic biomarker in non-small cell lung cancer. *Acta Oncol.* 2015;54(8):1113–9.

Paper II Karlsson T*, **Kvarnbrink S***, Holmlund C, Botling J, Micke P, Henriksson R, Johansson M, Hedman H. LMO7 and LIMCH1 interact with LRIG proteins in lung cancer, with prognostic implications for early-stage disease. *Lung Cancer.* 2018 Oct 2;125:174–84.

Paper III **Kvarnbrink S**, Hedman H, Johansson M. LRIG1 affects clonogenicity but not metastatic potential in non-small cell lung cancer cell lines. *Submitted manuscript.*

Papers I and II did not require permission to be reprinted.

Co-authored original papers not included in thesis

1. Asklund T, **Kvarnbrink S**, Holmlund C, Wibom C, Bergenheim T, Henriksson R, Hedman H. Synergistic killing of glioblastoma stem-like cells by bortezomib and HDAC inhibitors. *Anticancer Res.* 2012 Jul;32(7):2407–13.

2. Lindquist D, **Kvarnbrink S**, Henriksson R, Hedman H. LRIG and cancer prognosis. *Acta Oncol.* 2014 Sep;53(9):1135–42.

3. Mao F, Holmlund C, Faraz M, Wang W, Bergenheim T, **Kvarnbrink S**, Johansson M, Henriksson R, Hedman H. Lrig1 is a haploinsufficient tumor suppressor gene in malignant glioma. *Oncogenesis.* 2018 Feb 2;7(2):1–12.

4. Umapathy G, Wakil El A, Witek B, Chesler L, Danielson L, Deng X, Gray N, Johansson M, **Kvarnbrink S**, Ruuth K, Schönherr C, Palmer R, Hallberg B. The kinase ALK stimulates the kinase ERK5 to promote the expression of the oncogene MYCN in neuroblastoma. *Sci Signal.* 2014 Oct 28;7(349):ra102–2.

Abbreviations

ADC	Adenocarcinoma
ALK	Anaplastic lymphoma kinase
ATP, ADP	Adenosine triphosphate, adenosine diphosphate
BCA	Bicinchoninic acid
BED	Biologically effective dose
BMP	Bone morphogenetic protein
BRAF	Rapidly accelerated fibrosarcoma oncogene, homolog B
BRCA1	Breast cancer susceptibility protein 1
CBL	Casitas B cell lymphoma
CD28, CD80	Cluster of differentiation 28, Cluster of differentiation 80
CNS	Central nervous system
CTLA-4	Cytotoxic T cell lymphocyte associated protein 4
DNA	Deoxiribonucleic acid
EGF	Epidermal growth factor
EGFR	Epidermal growth factor receptor
EML4	Echinoderm Microtubule-associated protein-like 4
EQD2	Equivalent dose in 2 Gy fractions
ErbB	Erythroblastic oncogene B
ERCC1	Excision repair cross-complementing 1
FACS	Fluorescence activated cell sorting
FGFR1	Fibroblast growth factor receptor 1
FISH	Fluorescent enhanced *in situ* hybridization
GR	Growth rate
GTP, GDP	Guanoside triphosphate, guanoside diphosphate
HER2	Human epidermal growth factor receptor 2
Ig	Immunoglobulin
IHC	Immunohistochemistry
KIT	v-kit homolog kinase
KRAS	Kirsten rat sarcoma
LIMCH1	LIM and calponin homology domains protein 1
LMO7	LIM domain only protein 7
LRIG	Leucine-rich repeats and immunoglobulin-like domains
LRR	Leucine-rich repeats
MAPK	Mitogen activated protein kinase
MCS	Multiple cloning site

MEK	Mitogen activated protein kinase kinase
MET	Mesenchymal to epithelial transition
MRI	Magnetic resonance imaging
mRNA	Messenger ribonucleic acid (RNA)
NGS	Next generation sequencing
NSCLC	Non-small cell lung cancer
NTRK	Neurotrophin receptor tyrosine kinase
PBS	Phosphate buffered saline
PCR	Polymerase chain reaction
PD-1	Programmed death receptor 1
PD-L1	Programmed death receptor ligand 1
PDGFRα, PDGFRβ	Platelet derived growth factor receptor α and β
PI3K	Phosphoinositide-3 kinase
PIK3CA	Phosphatidylinositol-4,5-bisphosphate 3-kinase catalytic subunit alpha
PLA	Proximity ligation assay
Rb1	Retinoblastoma protein
RET	Rearranged during transfection protein
ROI	Region of interest
ROS1	C-ros oncogene 1
RRM1	Ribonucleoside reductase M1 subunit
RTK	Receptor tyrosine kinase
SBRT	Stereotaxic body radiotherapy
SCC	Squamous cell carcinoma
SCLC	Small cell lung cancer
siRNA	small interfering RNA
SISH	Silver-enhanced in situ hybridization
TBS	Tris-buffered saline
TCGA	The Cancer Genome Atlas
TKI	Tyrosine kinase inhibitor
TMA	Tissue microarray
TMB	Tumor mutational burden
TNM	[Primary] tumor, [lymph] node, metastasis (staging system)
TP53	Transformation-related protein 53
WHO	World Health Organization

Populärvetenskaplig sammanfattning på svenska

Lungcancer är den vanligaste enskilda orsaken till cancerrelaterad död såväl i Sverige som världen. Icke småcellig lungcancer är den dominerande formen, som indelas ytterligare i adenokarcinom och skivepitelcancer. En fjärdedel av patienterna med icke småcellig lungcancer som har lokalt växande små tumörer kan botas med enbart kirurgi ibland med tillägg av adjuvant cytostatikabehandling. Denna behandling har biverkningar och ökar chansen till bot med högst 5%. Fler biomarkörer behövs därför för att styra det kliniska beslutsfattandet vid de tidiga sjukdomsstadierna av icke småcellig lungcancer.

Proteinfamiljen LRIG består av tre liknande transmembranproteiner som samtliga är involverade i regleringen av tillväxtfaktorsignalering. LRIG1 är det mest studerade proteinet av dessa och interagerar med ett stort antal tillväxtfaktorreceptorer och andra relaterade proteiner. Höga nivåer av LRIG1 har kopplats till bättre överlevnad vid ett stort antal cancersjukdomar, inklusive bland annat bröstcancer, urinblåsecancer, livmoderhalscancer, melanom och primära hjärntumörer. Målet med detta forskningsprojekt var att utröna om detta gäller även för icke småcellig lungcancer, och att ytterligare karakterisera de biologiska funktionerna hos LRIG-proteiner vid denna sjukdom.

För att undersöka den kliniska betydelsen av LRIG-proteiner vid icke småcellig lungcancer immunfärgade vi en tissue microarray (TMA) innehållandes vävnadsprover från 347 kirurgiskt behandlade NSCLC-patienter i tidigt stadium, med antikroppar mot LRIG1, LRIG2 och LRIG3. Patienter med adenokarcinom och höga nivåer av LRIG1 befanns ha en stor och statistiskt signifikant överlevnadsfördel jämfört med negativa fall, och överlevde i medeltal 33 månader längre. En analys av genexpressionsdata i Oncomine-databasen visade även att högt genuttryck av *LRIG1* var kopplat till liknande överlevnadsfördelar. Skillnaderna i överlevnad kvarstod även efter justering för kända kliniska prognosfaktorer, vilket innebär att LRIG1 är en oberoende positiv prognostisk markör för överlevnad vid NSCLC.

En jäst två hybrid-screening utfördes för att leta proteiner som interagerade med ett evolutionärt bevarat proteinfragment som delas mellan alla LRIG-proteiner. Screeningen resulterade i träffar för de två närbesläktade proteinerna LMO7 och LIMCH1. LRIG1 och LRIG3 befanns båda interagera fysiskt med LMO7 och LIMCH1 vid immunprecipitation av överuttryckta proteiner. För

LMO7 och LRIG1 respektive LRIG3 kunde vi med metoden proximity ligation assay påvisa att interaktionen sker även vid endogent uttryckta proteiner. Vidare kunde vi påvisa i en överlevnadsanalys att LMO7 ensamt inte har någon prognostisk effekt, men att överlevnadsfördelen vi observerade för höga nivåer av LRIG1 enbart gäller för patienter som samtidigt inte har förekomst av LMO7 i tumörvävnad. Detta betyder att den påvisade interaktionen mellan LRIG1 och LMO7 även medför skillnader i överlevnad.

För att undersöka mekanismer bakom de påvisade skillnaderna i överlevnad, modifierade vi cellinjer etablerade från icke småcellig lungcancer till att överuttrycka LRIG1. I stort resulterade överuttryck av LRIG1 endast i mindre skillnader i celldelningstakt och inga nämnvärda effekter på cellernas känslighet för vare sig cytostatika eller strålning. Däremot ledde överuttryck av LRIG1 till signifikant minskad klonogenicitet i de flesta cellinjerna. Den enda cellinjen i panelen som visade sig ha förmågan att bilda hematogena mikrometastaser, H1299, användes för att etablera en mixad primärtumör där spårbara celler med överuttryck av LRIG1 blandats med spårbara kontrollceller. LRIG1 anrikades i den injicerade primärtumören enbart, men cellsammansättningen var oförändrad när metastaser jämfördes med sina respektive primärtumörer.

Sammanfattningsvis kom vi fram till att LRIG1 var en oberoende positiv prognostisk faktor i tidiga stadier av icke småcellig lungcancer. Vi identifierade LMO7 och LIMCH1 som nya interaktionspartners för LRIG-proteiner och visade att interaktionen mellan LMO7 och LRIG1 har direkt relevans för det kliniska utfallet i lungcancer. Vidare visar våra mekanistiska studier på överuttryck av LRIG1 i tumörceller att överlevnadsfördelen åtminstone delvis beror på skillnader i förmågan att metastasera. Sammantaget pekar fynden i denna avhandling mot att LRIG-proteiner kan vara av viktig betydelse vid icke småcellig lungcancer.

Introduction

More lives are lost each year to lung cancer, than to any other form of cancer. In 2018, 2.1 million people were estimated to have been diagnosed with lung cancer, and 1.8 million lung cancer patients were estimated to have died (1). In Sweden, the estimated figures were 4,000 new cases and 3,850 deaths (2) (Figure 1A). The disease is strongly linked to cigarette smoking and most estimates point toward 85% of all cases in the western world being smokers or former smokers (3). The lifetime risk of dying from lung cancer for a current smoker is estimated to be in the 15–20% range, but since the risk for acquiring the disease increases with the amount of tobacco exposure, the figure is as high as 30–40% for current heavy smokers at the age of 75 (4). Other major contributors, that to a large extent act synergistically with tobacco smoke in increasing the risk of lung cancer, are exposure to occupational carcinogens (9–15% of cases), radon (10%) and outdoor air pollution (1–2%) (5).

A quick comparison of the incidence and mortality figures reveals that the survival rate is lower than in most other high-incidence malignant diseases, and indeed, between 55 and 70 percent of new cases in the Western world do not survive past the first year (6). This is in part due to lung cancer frequently being diagnosed at a late stage; more than half of all new cases in Sweden have stage IV disease at the time of diagnosis, and less than a third are in disease stages I-II (Figure 1B) (7). Since no screening programs or similar efforts have been introduced, the distribution of clinical stage has not changed significantly over the years. The high mortality also means that the subgroup of never smokers, which may appear small by comparison, accounts for roughly as many cancer deaths per year as leukemia or esophageal cancer (3).

Lung cancer is subdivided into small cell lung cancer (SCLC) and non-small cell lung cancer (NSCLC). SCLC is a separate disease assumed to originate from neuroendocrine cells in the lung, has very little in common with NSCLC with regards to treatment as well as tumor biology, and is thus not included in the scope of this thesis. NSCLC is further subdivided into adenocarcinoma (ADC), squamous cell carcinoma (SCC) and undifferentiated NSCLC (8). Adenocarcinoma is presumed to originate from epithelial cells in the alveoli or respiratory bronchiole, whereas SCC originates from respiratory epithelium in larger airways undergoing squamous metaplasia; centrally located tumors

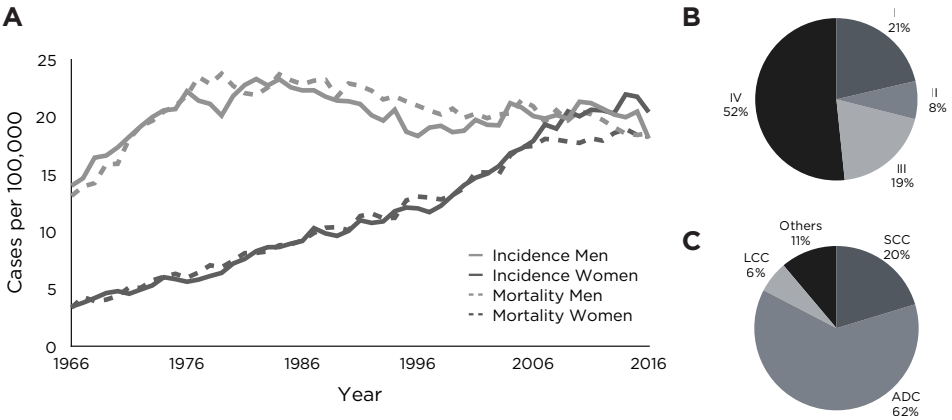

Figure 1. *Basic epidemiology of NSCLC in Sweden.* (**A**) Incidence and mortality. Statistics collected from the NORDCAN and SCB databases, covering 50 years up until the most recent year with complete statistics (2016). Shown are line diagrams separated by sex. Solid lines representing incidence, dashed lines representing mortality. (**B**) Distribution of clinical stage and (**C**) major histological subtypes in Swedish NSCLC cases diagnosed between 2015 and 2019. Data collected from the Swedish lung cancer registry. ADC = adenocarcinoma, SCC = squamous cell carcinoma, LCC = large cell carcinoma.

are more common when compared to ADC. In the late 1900s, a histological transition occurred in which ADC overtook SCC as the predominant subtype, presumably due to changes in cigarette composition (5,9,10), and more than half of all NSCLC cases in Sweden are currently adenocarcinomas (Figure 1C).

Treatment by clinical stage

In Sweden, lung cancer is treated according to a national care program, which largely reflects the international consensus. In general terms, surgery is used when possible, and medical treatment improves the outcome in all clinical stages. Treatment options are entirely dependent on clinical stage, which, in turn, is based on primary tumor status, nodal involvement and distant metastasis according to the TNM system (11). An overview of TNM staging and translation to clinical stage is shown in Table 1– 2.

	0	1	2	3	4
Primary tumor (T)	T0: no evidence of tumor Tis: carcinoma in situ	≤ 3 cm T1a: ≤ 1 cm T1b: >1 to ≤2 cm T1c: >2 to ≤3 cm	> 3 to ≤ 5 cm T2a: >3 to ≤4 cm T2b: >4 to ≤5 cm or involvement of main bronchus, limited atelectasis etc.	> 5 to ≤ 7 cm or atelectasis of whole lung, multiple nodules in same lung, invasion of chest wall, diaphragm	> 7 cm Invasion of heart, large vessels, trachea, esophagus, etc.
Lymph nodes (N)	None	Intrapulmonary nodes, ipsilateral peribronchial or perihilar	Ipsilateral mediastinal or subcarinal nodes	In supraclavicular fossa or scalene. Anything on other side of midline.	
Metastases (M)	None	M1a: contralateral lung, pleural nodules, malignant pleural effusion M1b: single extrathoracic metastasis M1c: multiple extrathoracic metastases			

Table 1. A simplified summary of TNM staging in NSCLC. Adopted after TNM8, The Union for International Cancer Control (UICC).

Localized disease — stage I and II

Surgery by means of lobectomy or pneumonectomy is the preferred option for curative treatment in disease stages Ia through IIb. From disease stage Ib and upwards, adjuvant chemotherapy with a platinum-based combination regimen is offered in order to prevent disease recurrence and the development of metastatic disease. A cisplatin and vinorelbine doublet has been associated with a slight survival benefit compared to other regimens in clinical studies and is therefore the regimen of choice in most cases. The survival benefit of adjuvant chemotherapy is 4–6% over 5 years (12,13), which unfortunately also means that the majority of patients receive a relatively toxic treatment without

	N0	N1	N2	N3
T1	Ia	IIb	IIIa	IIIb
T2a	Ib	IIb	IIIa	IIIb
T2b	IIa	IIb	IIIa	IIIb
T3	IIb	IIIa	IIIb	IIIc
T4	IIIa	IIIa	IIIb	IIIc
M1a	IVa	IVa	IVa	IVa
M1b	IVa	IVa	IVa	IVa
M1c	IVb	IVb	IVb	IVb

Table 2. Translation of TNM stages to clinical stages in NSCLC (TNM8, UICC).

improvements in survival. Biomarkers for better selection of adjuvant therapy are much needed, and the development of biomarkers to predict risk for metastatic disease could possibly lead to higher cure rates as well as fewer patients being treated without benefit.

Due to the fact that most patients are current or former smokers, the patient group has abundant cardiovascular and pulmonary co-morbidity, which may limit the treatment options. Early-stage patients that are inoperable due to heart disease or impaired lung function may be offered stereotaxic body radiotherapy (SBRT) given in three 15 Gy fractions, to an equivalent dose in 2 Gy fractions ($EQD2_{10}$) of 93.8 Gy, or radiochemotherapy. Since the degree of disease control appears comparable to that of surgery (14), multi-center trials in which early-stage patients are randomized to either surgery or SBRT are currently underway.

Locally advanced disease — stage III

Locally advanced disease is also treated with a curative intent when possible. The first hand choice for stage III patients is concomitant radiochemotherapy with a platinum-doublet regimen in conjunction with radiotherapy, to a total dose of 66–68 Gy given in 2 Gy fractions (15,16). Radiochemotherapy alone gives a 5-year survival in the 15–30% range, with an estimated median survival of 28 months (17). Recently, the programmed death receptor ligand 1 (PD-L1)

blocking antibody durvalumab was approved for use after radiochemotherapy, resulting in significantly higher two-year survival rates that translate into higher cure rates as well (18,19). Curative surgery can be performed on stage IIIA patients with limited and ipsilateral nodal involvement, but is limited to select cases, often results in non-radical R1 or R2 resections (17), and provides no significant survival benefit compared to radiochemotherapy (20).

Metastatic disease — stage IV

Unlike the curable stages I through III, treatment in stage IV NSCLC is highly dependent on molecular features and incorporates a wide range of medical treatments as well as palliative radiotherapy. According to the Swedish standard of care, cases of stage IV lung adenocarcinoma are screened at the time of diagnosis for epidermal growth factor receptor (EGFR) and rapidly accelerating fibrosarcoma homolog B (BRAF) mutations by means of polymerase chain reaction (PCR) or next generation sequencing (NGS), anaplastic lymphoma kinase (*ALK*) and c-ros oncogene 1 (*ROS1*) gene rearrangements using immunohistochemistry (IHC) and split-probe fluorescent/silver-enhanced in situ hybridization (FISH/SISH), and assessed for PD-L1 expression using IHC. Squamous cell carcinomas are evaluated for PD-L1 expression and mutation screened using NGS. Biomarker data is then used in the clinical decision making, and patients with positive outcome on the treatment predictive analyses are typically offered the corresponding targeted therapy as a first line treatment. The molecular specifics of those targeted therapies and their corresponding biomarkers are discussed further down, in the section on molecular features.

The majority of stage IV patients are currently not eligible for any targeted therapies as a first line treatment due to unfavorable biomarker status. Of these, a majority are still in a general condition that allows for medical treatment, *i.e.* having a World Health Organization (WHO) performance status of 2 or less. These patients are offered palliative immunochemotherapy, immunotherapy alone or in some cases chemotherapy alone. Chemotherapy is usually based on similar platinum doublet regimes as in the adjuvant or curative setting. Alternatively, for fragile patients, vinorelbine, gemcitabine or pemetrexed monotherapy may be used instead. Almost regardless of eligibility for medical therapy, palliative radiotherapy can be used for local control and symptom relief. Primary tumors are irradiated with a dose in the BED_{10} range of 50 Gy,

typically 36–39 Gy given in 3 Gy fractions, which slightly improves survival (21), or 20 Gy in 4 Gy fractions for symptomatic control. Metastases are irradiated with anything from single 8 Gy fractions for pain relief to 20–30 Gy in 3–5 Gy fractions for local control and debulking.

Medical treatment

Chemotherapy

The clinical use of chemotherapy alone in NSCLC has decreased with the advent of targeted therapies and immunotherapy, but remains of importance in combined regimens with radiotherapy in the curative setting and immunotherapy in the palliative setting. The regimens of choice are platinum-based doublets in which cisplatin or carboplatin is combined primarily with a chemotherapeutic drug with another mechanism of action, most often vinorelbine or pemetrexed. Platinum salts act by distorting the DNA tertiary structure (22), making it impossible to replicate, and the addition of a secondary cytotoxic mechanism potently forces cells into apoptosis or necrosis when replicating. For NSCLC, the commonly used drugs are microtubule inhibitors (vinorelbine, docetaxel, paclitaxel) and antimetabolites (pemetrexed, gemcitabine).

Tyrosine kinase inhibitors

Tyrosine kinase inhibitors (TKIs) have been in routine use for the treatment of NSCLC since 2004, when the first EGFR TKIs were approved for use. TKIs are orally available small molecules designed to inhibit the kinase domain of single or multiple receptor tyrosine kinases (RTKs), either by binding to the adenosine triphosphate (ATP) binding pocket, a conserved catalytic loop of the tyrosine kinase domain or less conserved structures more specific to a single RTK (23). Most of these small molecule inhibitors bind reversibly, while some of the most recently developed drugs are covalently linked to their target regions, which delays the development of TKI resistance (24-26). The TKIs used in the treatment of NSCLC bind to quite specific regions on single RTKs and inhibit their activity potently with few off-target effects, which also means that TKI treatments for NSCLC are useless without the verified presence of certain activating mutations, which are discussed in a later chapter.

The TKIs currently used in NSCLC are designed to target EGFR, ALK, ROS1, the mesenchymal to epithelial transition kinase (MET), BRAF and mitogen-activated protein kinase kinase (MEK). The EGFR inhibitors most commonly used are afatinib, dacomitinib and osimertinib, which are second and third generation EGFR TKIs with good penetrance into the central nervous system (CNS) and longer median times to treatment resistance compared to first generation TKIs such as gefitinib and erlotinib. Side effects are mostly related to disturbed turnover of certain epithelial tissues, with diarrhea and acne vulgaris like rashes being the most common issues. For *ALK* rearrangements, the second generation TKIs, alectinib and brigatinib, are most commonly used in the first line setting, also due to CNS penetrance and more lasting responses (27,28). The first generation ALK TKI, crizotinib, is the only currently approved drug that inhibits ROS1 and MET. The BRAF TKI dabrafenib is approved for use in NSCLC, but only in combination with the MEK TKI trametinib, as dabrafenib itself has activating off-target effects on the downstream MEK kinase that need to be inhibited to avoid paradoxical effects.

Immunotherapy

Earlier trials on non-specific immune activators, such as interferon and high-dose interleukin 2 treatment, had considerable side effects and very poor results (29). However, in the late aughts, a trial on ipilimumab, a novel cytotoxic T cell lymphocyte associated protein 4 (CTLA-4) inhibitory antibody, showed a considerable effect on stage IV melanoma patients (30), essentially marking the beginning of a new era in medical oncology. CTLA-4 is a co-inhibitory T cell receptor that competes with a co-stimulatory receptor, cluster of differentiation 28 (CD28), for binding to ligands CD80 and CD84 during antigen presentation (31,32). Thus, CTLA-4 blockade leads to massive T cell activation. Since it is expressed on regulatory and early activated T cells, CTLA-4 blockade is associated with autoimmune side effects that, in some cases, may be life-threatening (33,34). Ipilimumab has been used as part of a double blockade combination immunotherapy in clinical trials with some promising results (35,36), but is not yet used routinely in the treatment of NSCLC.

Mostly due to the aforementioned side effects in relation to the therapeutic effect of CTLA-4 blockade, research focus soon shifted to another immune checkpoint, consisting of the programmed death 1 (PD-1) receptor and its membrane-bound ligand, programmed death ligand 1 (PD-L1). PD-1 is structurally

Score	Description
0	Fully active, able to carry on any pre-disease performance without restriction.
1	Restricted in a physically strenuous activity but ambulatory and able to carry out work in a light or sedentary nature, *e.g.* light house work or office work.
2	Ambulatory and capable of all self-care but unable to carry out any work activities. Up and about more than 50% of waking hours.
3	Capable of only limited self-care, confined to bed or chair more than 50% of waking hours.
4	Completely disabled. Cannot carry on self-care. Totally confined to bed or chair.
5	Dead.

Table 3. WHO Performance Status scale.

related to CTLA-4, and in a similar fashion, the PD-1/PD-L1 interaction occurs as a co-inhibitory mechanism in parallel to antigen presentation, but with the difference that PD-L1 is inducible and negatively regulates the response of T cells that are already engaged in an effector T cell response (37). Ligand binding results in phosphorylation of a C-terminal immune tyrosine-based inhibitory motif, recruiting Src homology region 2 domain-containing phosphatase 1 (SHP-1) and SHP-2 (38), as well as upregulation of ubiquitin ligases Casitas B cell lymphoma B (CBL-b) and c-CBL, both leading to T cell receptor down-modulation through various pathways (39). Since this occurs in the tumor itself, ectopic expression of PD-L1 is a method of immune evasion often employed by tumor cells (32). Blockade can occur on either PD-1 itself or PD-L1 and several antibodies for either target are already approved for clinical use. Blockade results in a vastly increased T cell activation upon antigen presentation, resulting in an intratumoral immune response with milder systemic side effects (40). Immunotherapy using PD-1/PD-L1 antibodies is today the mainstay of modern medical treatment of NSCLC without druggable driver mutations. Most patients are offered immunotherapy in combination with chemotherapy (41-43) or immunotherapy alone if tumor PD-L1 expression is >50% (44) as first line treatment.

Prognostic factors

Prognostic factors, by definition, determine the risk of a disease outcome (in this case, death), regardless of treatment and are therefore important in guiding the clinical decision making. Clinical stage is the single most important prognostic factor in NSCLC, always overshadowing the impact of other contributing factors; it is simply worse to be diagnosed with stage III disease than stage II or I disease, no matter what. That defines stage as an independent prognostic factor. Within stage categories, age (with a cut-off at 70 years) is prognostic, as is smoking status, with current smokers always having a worse prognosis than former smokers and never-smokers. However, there appears to be no difference in prognosis between former smokers and never-smokers. Male gender and squamous histology are both factors that are prognostically beneficial in stage Ia, but not in other disease stages (45).

Performance status, as measured by the WHO performance score (WHO PS, Table 3) (46), is another prognostically important factor with a large impact on survival as well as a key role in clinical decision making. It is even likely to have a larger prognostic impact than clinical stage, even though a direct comparison between the two factors was not possible due to limited datasets at the time when the staging systems were devised (45). WHO PS also acts as a helping factor in determining whether a patient is fit for treatment, as chemotherapeutic regimens generally are contraindicated at PS 3 or higher whereas targeted TKI treatments may provide a dramatic symptom relief even for a bedbound patient with a WHO PS of 4.

Molecular prognostic markers

There are several molecular markers that have been identified as independent prognostic markers for survival in retrospective studies. Generally, all such markers have also been proposed as predictive markers for sensitivity to chemotherapy, and those aspects of these biomarkers are discussed in detail in the next chapter. Briefly, the expression of excision repair cross-complement group 1 (ERCC1) and the ribonucleoside reductase M1 subunit, encoded by the *RRM1* gene, correlate with each other and the expression of both in tumor tissue was associated with longer survival in surgically treated NSCLC in a retrospective study (47). Using similar methodologies, favorable outcomes were observed for the breast cancer susceptibility protein 1 (*BRCA1*) expression (48) and high levels

of β-III tubulin expression (49). All the mentioned markers were considered promising enough to warrant prospective studies that came out negative, and the prognostic benefits described in the retrospective studies were generally not observed in those studies either (50).

Attempts have also been made at establishing gene signatures as prognostic markers in NSCLC. One signature based on five genes predicted survival in two retrospective datasets (51), and a 14-gene signature proposed by Kratz *et al.* have shown prognostic effects within clinical stages, yet again in retrospective studies (52). A 15-gene signature was developed as part of the JBR.10 trial and also showed potential for use as a prognostic marker in retrospectively collected data (53), but attempts to validate those results have been discordant (54).

Mutations in the Kirsten rat sarcoma gene (*KRAS*), which have been identified as tumor drivers in 25% of all NSCLC cases (55), might be regarded as prognostic factors at the present time. The KRAS protein is an intracellular messenger that binds guanoside triphosphate (GTP) or guanoside diphosphate (GDP). The protein is switched from its inactive GDP-bound state to an active GTP-bound state by upstream actor enzymes in the signaling cascade, which triggers downstream mitogenic signaling. Amino acid substitutions at position 12 or 13 result in the protein being stuck in an active GTP-bound state (56). Worse outcomes for cases harboring *KRAS* mutations have been reported in advanced disease (57,58), but the effect sizes were small. There is no targeted therapy for activating KRAS mutations approved for clinical use today. However, sotorasib, a small molecule capable of inhibiting $KRAS^{G12C}$, the most common activating KRAS mutation in NSCLC, is currently undergoing early clinical trials on late stage NSCLC patients (59). If favorable therapeutic effects are observed, and if drugs targeting additional common *KRAS* mutations are developed, oncogenic *KRAS* mutations may make the transition from weak negative prognostic markers to strong predictive markers.

Predictive markers for chemotherapy

As the limited benefit of adjuvant chemotherapy has been a known problem in the management of NSCLC for a long time, the idea of having molecular markers identifying the chances for an individual patient to have a higher or lower response to particular classes of chemotherapeutic drugs, or even to any kind of chemotherapy, has been attractive. Several studies have been performed

to investigate whether any clinical prognostic factors also predict sensitivity or resistance to certain chemotherapeutic drugs, but the only predictive effect that has ever been shown in prospective studies is that squamous histology predicts poor response to pemetrexed (50).

The most studied proposed predictive molecular marker for chemosensitivity is ERCC1, which is the rate-limiting enzyme involved in the nucleotide excision repair complex, which can reverse the DNA damage induced by platinum salts. Effects on cisplatin sensitivity has been shown mechanistically using ectopic overexpression of *ERCC1* in various malignant cell lines (60), and a retrospective study showed better outcome for patients with low *ERCC1* expression that were treated with cisplatin (61,62). The *RRM1* gene, involved in reduction of the nucleotides that gemcitabine competes with in DNA synthesis, has been investigated in the same context. The expression of *RRM1* was therefore hypothesized to predict response to gemcitabine, which was supported by experimental studies on a colon cancer mouse model (63) and findings from retrospective studies on a surgically treated cohort (64). Based on these results, a clinical trial was designed, in which patients received adjuvant combination chemotherapy tailored to their individual expression of *ERCC1* and *RRM1* in tumor tissue (65). The results were negative; *ERCC1* high-expressing cases did not have a worse response to carboplatin, and *RRM1* high-expressing cases did not have a worse response to gemcitabine. The mechanics of ERCC1 have also shown to be complicated, as only one isoform out of four is actually involved in DNA repair (66).

The BRCA1 protein is also a player in nucleotide excision repair that has been hypothesized to confer resistance to cisplatin, possibly in conjunction with ERCC1 (67), and studies on retrospective data indicated that high levels could predict platinum resistance (68), as well as sensitivity to microtubule inhibitors (69). Again, a phase III clinical trial using *BRCA1* expression for biomarker-directed chemotherapy showed no improved outcome (70). Similarly, levels of β-III tubulin were proposed to predict resistance to taxane based chemotherapy (71), but no predictive effect was observed in prospective studies (72).

In retrospect, the mentioned biomarkers definitely do have important biological effects in NSCLC, as well as in other human cancers. However, a possible conclusion from the many performed studies is that chemosensitivity is conferred by multiple interacting factors and, therefore, may not predictable by single biomarkers.

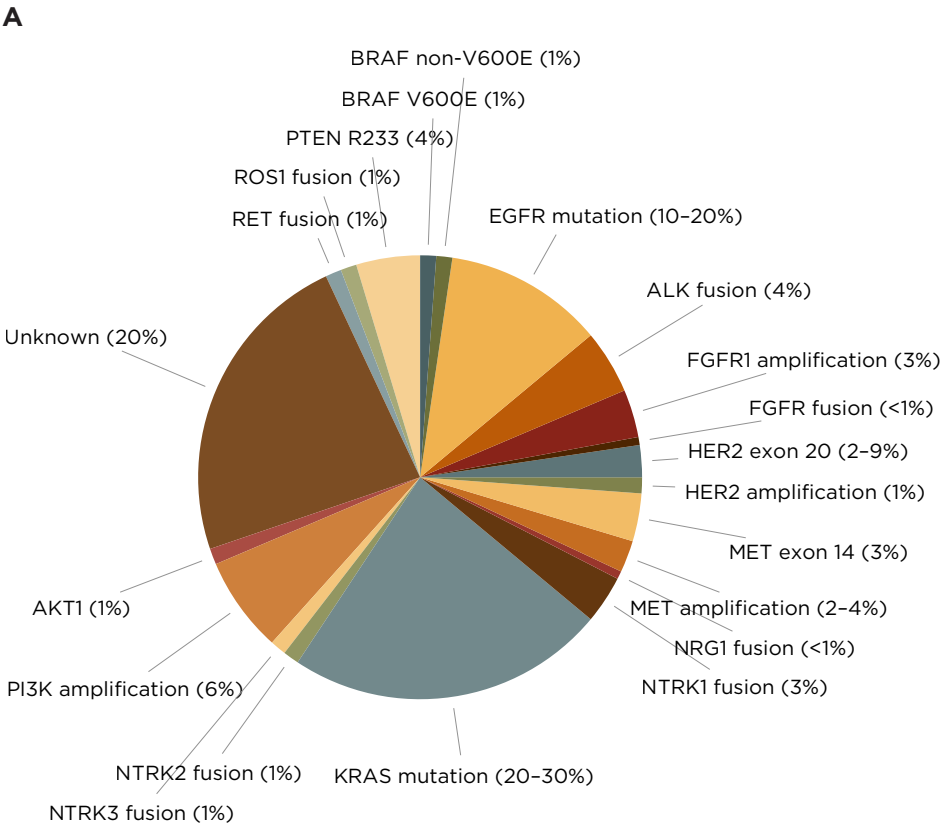

Figure 2. *Oncogenic mutations in NSCLC.* (**A**) Frequency distribution of identified oncogenic driver mutations in NSCLC. Adapted from Barlesi *et al.* (2016) and Cho (2018). (**B**) Approximate distributions of current NSCLC driver mutations that are druggable using substances approved for NSCLC (FDA approved), approved for other diseases but not NSCLC (Off-label druggable) and non-druggable.

Predictive markers for targeted therapies

Thanks to advances in high-throughput sequencing, the genetic categorization of NSCLC has greatly evolved during the past decade, and the previously dominating subset of tumors with unknown driver mutations now constitutes less than 20% of NSCLC cases (73-76), summarized in Figure 2. Of the currently non-targetable genomic alterations, amplification of the fibroblast growth factor receptor 1 gene (*FGFR1*) is seen in ~20% of all cases, almost always with SCC histology, and with a strong link to smoking (77-79). Activating *KRAS* mutations, resulting in amino acid substitutions at positions 12, 13 or 61, are seen in ~25% of all cases, mainly adenocarcinomas, also with a strong link to smoking (80). Currently, the targetable genomic alterations consist of *EGFR* mutations, exon 14-skipping mutations in the *MET* gene, activating *BRAF* mutations, and *ALK* and *ROS1* rearrangements. Those alterations are, with very few exceptions, mutually exclusive with each other, as well as with *KRAS* mutations, which means that each of these driver mutations can be regarded as a distinct molecular subtype (81,82). Apart from the above-mentioned genetic drivers, there are several others, such as *MET* amplifications and mutations & amplifications in the erythroblastic oncogene B2 (*ERBB2*) gene, that may be off-label druggable with already approved substances. A subset of NSCLC patients display neurotrophin receptor tyrosine kinase (NTRK) gene fusions where larotrectinib is approved (83). RET fusions are present in 1–2% of NSCLC cases and may be targeted with approved TKIs such as cabozantinib, lenvantinib or sorafenib. Promising results for the specific RET inhibitor selpercatinib have recently been presented (84) and approved for NSCLC in the US by the Food and Drug Administration (FDA).

EGFR

The epidermal growth factor receptor (EGFR), also known as ErbB1, is a receptor tyrosine kinase (RTK) in the ErbB family that consists of an extracellular domain with a ligand binding pocket with affinity for the epidermal growth factor (EGF) and closely related ligands, a transmembrane domain, and a cytosolic domain containing an ATP binding pocket and a tyrosine kinase subunit (85). Ligand binding causes the protein to form dimers with ErbB family members (Figure 3), and the cytosolic domains in the dimerized complex then phosphorylate specific tyrosine residues on the dimerization partner. In turn, the phosphorylated residues attract different downstream signaling actors, which

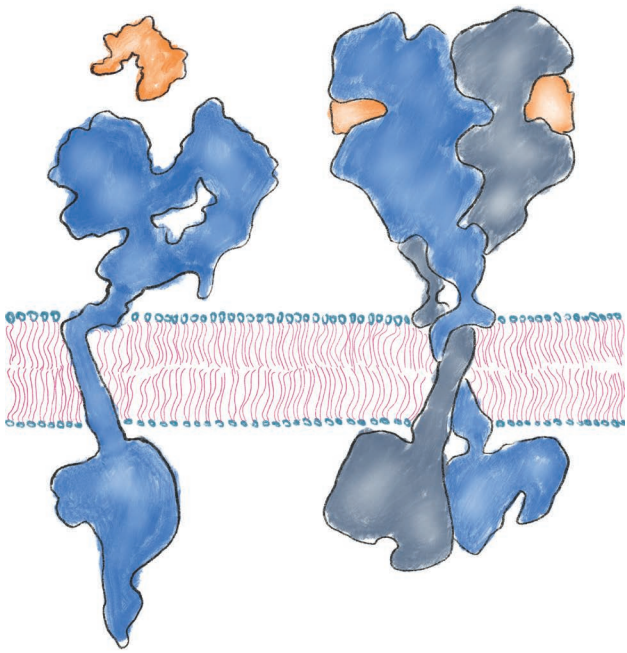

Figure 3. *EGFR structure.* EGFR in its monomeric form *(left)* is inactive. When the ligand, EGF (in orange), is bound, EGFR assumes its active conformation and dimerizes with proteins in the ErbB family. The intracellular kinase domain becomes accessible in the active conformation, resulting in activating phosphorylation of downstream messenger proteins. Shown is an active EGFR homodimer *(right)*.

leads to activation of their corresponding signaling pathways (86), including the well-known mitogen activated protein kinase (MAPK) and phosphoinositide-3 kinase (PI3K) signaling pathways. EGFR dimerization preferentially occurs with the ligand-less and kinase active ERBB2, most commonly known as human epidermal growth factor receptor 2 (HER2), which results in increased EGF ligand affinity and prolonged time in active conformation (87,88), but EGFR-EGFR homodimers as well as other ErbB heterodimers can also be formed, providing a level of signaling diversification since other tyrosine residues are phosphorylated (86).

The EGFR protein and its corresponding gene were cloned and characterized in the beginning of the 1980s (85,89,90), and their clinical importance in NSCLC was unraveled in parallel with their discovery (91-93). This resulted in a race to develop anti-EGFR treatments for use in lung cancer, that in retrospect predated the discovery of their corresponding biomarkers. In the mid-2000s, during a retrospective tumor genomics analysis of non-responders to first generation EGFR TKIs, the first NSCLC-specific driver mutations in the *EGFR* gene were discovered, which finally provided the means of predicting response

to anti-EGFR therapy (94-96). These mutations all affect the EGFR kinase domain, resulting in increased ligand-dependent signaling due to an abnormally stable active conformation (97). This increased signaling has downstream effects on hallmark features, resulting in increased proliferation, invasion & cell migration, and evasion of apoptosis (98). Patients with activating *EGFR* mutations often have a marked response to treatment (94), but resistance often develops within months. EGFR TKI resistance occurs either through an acquired resistance-conferring mutation in *EGFR* itself, activation of other driving RTKs, known as a kinase switch, or a phenotypic switch to SCLC.

In approximately 50% of cases with acquired TKI resistance, a threonine to methionine substitution at position 790 (T790M) is detected, which expands by selective pressure under treatment. T790M is in itself a targetable mutation, using irreversibly binding third generation TKIs such as osimertinib (99). In 1–2% of TKI resistant cases, resistance is conferred by other EGFR amino acid substitutions, also targetable using third generation TKIs (100), but there are tertiary mutations described that confer intrinsic resistance to third generation TKIs as well (101). Kinase switch to MET signaling occurs through amplification of the gene encoding for the receptor itself or its ligand (102-104). Similarly, a HER2-driven subpopulation can occur through amplification of the *HER2* gene (105), and a switch to AXL signaling is mediated through receptor or ligand gene amplification (106). EGFR TKI resistance through phenotypic switch to SCLC is associated with pre-existing or acquired transformation-related protein 53 (*TP53*) and retinoblastoma protein (*RB1*) mutations (107) along with acquired phosphatidylinositol-4,5-bisphosphate 3-kinase catalytic subunit alpha (*PIK3CA*) mutations, even though the actual mechanism of transformation is currently unknown. SCLC transformation typically confers sensitivity to the standard SCLC treatment regimen with cisplatin and etoposide (103,108).

ALK and ROS1

ALK is an RTK that was originally discovered as a tumor driving fusion partner in anaplastic large cell Hodgkin lymphoma, hence the name. Under normal conditions, ALK is only present in embryonal tissues, in which binding of its ligands results in oligodimerization of the tyrosine kinase domain and downstream activation of the MAPK and PI3K pathways (109-111). Multiple other pathways have been described in mechanistic studies of oncogenic fusion proteins (112,113). In 2007, it was discovered that a gene fusion between

Echinoderm microtubule-associated protein-like 4 (*EML4*) and *ALK* acts as a tumor driver in 4–5% of NSCLC cases (114,115). The resulting gene fusion, *EML4-ALK*, encodes a hybrid protein with ligand-independent dimerization and activation of the ALK catalytic domain. More than 10 different EML4-ALK fusion variants have been characterized, all with highly potent oncogenic effects *in vivo* as well as *in vitro* (116-118). Clinically, *ALK* rearrangements are seen in adenocarcinomas and preferentially occur in younger patients with less tobacco exposure (73).

Shortly after the discovery of *ALK* rearrangements as drivers in NSCLC, it was shown that ROS1, an orphan RTK with a high degree of sequence homology to ALK, also could be present in oncogenic fusion proteins (119), acting as an oncogenic driver in approximately 1% of NSCLC cases (120). Multiple *ROS1* fusion partners are described, all resulting in activated ROS1 signaling (121,122).

The kinase domains of ALK and ROS1 are highly similar, and both are potently inhibited by the multi-kinase inhibitor crizotinib, which binds near the ATP binding pocket and disables the kinase activity. However, resistance occurs in a similar fashion as with EGFR, primarily through the development of acquired point mutations, kinase switch or phenotypic change. Multiple resistance-conferring amino acid substitutions have been described and act in a similar way as the secondary EGFR mutations (123-125). Second and third generation TKIs, binding to other sites in the catalytic domain, delay the development of TKI resistance (27,28) and are currently approved for clinical use in ALK rearranged NSCLC. Kinase switch is seen in ALK or ROS1 rearranged NSCLC as well, to either the v-kit homolog kinase (KIT) or EGFR (124). At least for ALK positive tumors, a phenotypic switch to SCLC may occur as well (113,126).

MET

The MET protein is an RTK that is activated through binding of its ligand, the hepatocyte growth factor. Activation results in downstream signaling through multiple pathways, including the MAPK and focal adhesion kinase (FAK) pathways, resulting in cellular proliferation, motility and invasion (127). In approximately 3% of NSCLC cases, skipping alterations in exon 14 of the *MET* gene act as tumor drivers. The exon 14-skipping mutations result in a functional MET protein that lacks a binding site for the CBL E3 ubiquitin ligase, that

normally flags the protein for proteasomic degradation, and the end result is a massive enrichment of the receptor at the cell surface (128). The MET kinase domain has conserved domains in common with ALK and ROS1, including the crizotinib binding site. Generally, NSCLC cases harboring a *MET* exon 14 skipping mutation respond to crizotinib therapy, but with lower response rates than *ALK* rearranged tumors (129).

BRAF

The BRAF protein is a member of the MAPK signaling pathway, acting downstream of KRAS and, in turn, phosphorylating the mitogen activated protein kinase kinase (MEK). Given its central role in mitogenic signaling, its function has been well known for a long time. In the field of cancer, activating *BRAF* mutations were mostly known as a key player in melanoma (130), but they have recently been identified as driver mutations in 2% of NSCLC cases as well (73,131). As in melanoma, a valine to glutamic acid substitution at position 600 (V600E) is the most common single mutation, seen in 50% of cases, disrupting an interacting loop that is assumed to stabilize the inactive conformation. Other mutations of unknown mechanistic importance, such as G469A or D594G, are present at a higher frequency than in melanoma (131). Strikingly, the patient characteristics are different compared to *EGFR* mutated or *ALK/ROS1* rearranged cases in that the frequency of never smokers is considerably lower. As with the other driver mutations, there is very little to no overlap between *BRAF* mutations and *EGFR* mutations or *ALK/ROS1* rearrangements.

Predictive markers for immunotherapy

The tumor mutational burden (TMB) in NSCLC is among the highest among all human cancers, second only to melanoma (132), meaning that many tumors are assumed to express altered peptide sequences (neoantigens) that are recognized as foreign by the adaptive immune system.

Judging from the mechanism of action, one might hypothesize that PD-L1 expression in tumor cells is a predictive marker for immune checkpoint blockade, but this is only partly the case as less than half of PD-L1 positive tumors respond to PD-L1 blockade (44). Despite that, PD-L1 is currently the only biomarker used in the clinical decision making regarding immunotherapy in

NSCLC. PD-L1 positivity in tumor tissue is quantified using the proportion of IHC positive tumor cells, with a cut-off value of ≥50% for first line monotherapy use and 0-1% for second line use in stage IV disease, and 1% for adjuvant use of durvalumab in stage III disease.

Theoretically, the best predictive biomarker would be the actual amount of neoantigens in tumor tissue, but this is unfeasible since it would require the specific detection of random, unknown peptide sequences. A rational approach is to measure TMB rather than the actual neoantigens, since the former is a prerequisite for the latter and thereby functions as a surrogate marker. Most clinical studies and proposed clinical implementations measure TMB by means of high-throughput hybrid next-generation sequencing platforms that report the number of mutations per million bases. In retrospective studies, TMB as measured in this way has been considerably more predictive of treatment response than PD-L1 IHC positivity (133,134). However, in prospective clinical trials, the importance of TMB has not been validated (135).

Another key point, besides PD-L1, is that the presence of single drivers such as *EGFR* mutations and *ALK* or *ROS1* rearrangements, is a strong negative predictive marker for all current immunotherapies for NSCLC, even though they often have high PD-L1 expression (136,137). This is in line with the low TMB reported for these subsets of tumors (138), and further underlines the fact that PD-L1 in itself is an insufficient biomarker for treatment response.

LRIG proteins

The leucine-rich and immunoglobulin-like (LRIG) protein family consists of the paralogous transmembrane proteins LRIG1, LRIG2 and LRIG3, encoded by correspondingly named genes located at chromosome 3p14, 1p13.1 and 12q14.1, respectively. They have a common structure featuring an N-terminal signal peptide, 15 tandem leucine-rich repeats (LRRs) with cysteine rich flanking domains at the N- and C-terminal ends, three membrane proximal immunoglobulin-like (Ig) domains, a transmembrane domain and a C-terminal cytosolic domain (139) (Figure 4). Despite LRRs and Ig domains being relatively common in the human proteome, generally with roles in protein-protein interactions, proteins harboring both domains is a bit of an oddity that is mostly seen in the LRIG and amphoterin-induced (AMIGO)/Alivin protein families (140). The amino acid sequence is 41.8% identical between LRIG1 and LRIG2, and

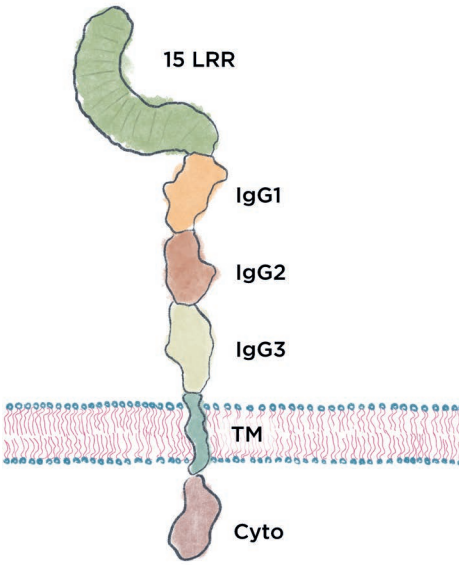

Figure 4. *Approximative LRIG1 structure.* LRIG1 has an extracellular domain containing 15 leucine-rich repeats (LRRs) and three Ig domains (IgG1–IgG3), a transmembrane domain (TM) and a cytosolic domain (Cyto). The structure of the extracellular domain, but not the other domains, has been characterized through X-ray crystallography. Shown is a rendition of the full-length protein.

46.8% identical between LRIG1 and LRIG3. Orthologs for all three proteins exist in vertebrates; for instance, mouse Lrig1 is 80.1% sequence identical to human LRIG1, while non-vertebrates generally have a single LRIG ortholog (139). Of these, the most studied ortholog is Sma-10 in *Caenorhabditis elegans* (141).

The LRIG proteins share a common functional theme as they physically interact with RTKs and modulate their signaling. LRIG1 is the first discovered and most studied member, and has been found to interact in an inhibitory fashion with all ErbB family members (EGFR, ERBB2, ERBB3 and ERBB4) (142,143), MET (144), rearranged during transfection protein (RET) (145), platelet-derived growth factor receptor alpha (PDGFRα) (146) and NTRK2 (147), predominantly by promoting lysosomal degradation of its targets (142-144,148). The inhibitory effects on EGFR have not only been observed *in cis*, but also *in trans* as the extracellular domain of LRIG1 is shed and inhibits EGFR signaling on nearby cells (149), which has been harnessed therapeutically in a rat glioma model (150). Interestingly, the *C. elegans* LRIG ortholog, SMA-10, binds to and enhances the downstream signaling of bone morphogenetic protein (BMP) receptor orthologs even though they aren't tyrosine kinases (141), and Lrig1 has been shown to modulate BMP signaling in mouse cells as well (Herdenberg, unpublished observations). Given its well documented role in

endogenous down-regulation of growth factor signals, it is not surprising that LRIG1 has been associated with better survival in cancer — high expression of LRIG1 in tumor tissue, measured either through gene copy number, mRNA levels or protein levels, has been linked to better prognosis in bladder cancer (151), breast cancer (152-154), both subtypes of cervical cancer (155,156), cutaneous squamous cell carcinoma (157), high-grade glioma (151), head and neck squamous cell carcinoma (158,159), hepatocellular carcinoma (160) and malignant melanoma (151). Furthermore, absence of *Lrig1* in knockout mice leads to increased Egfr and Met signaling in tissues (161,162), with a phenotype characterized by psoriasiform hyperproliferative lesions on the skin (163), an enlarged intestine due to hyperproliferation of the intestinal epithelium (161), and spontaneous development of duodenal carcinomas at an early age (162), which means that it acts as a proper tumor suppressor.

LRIG2 and LRIG3 are less extensively studied, both with regards to their mechanisms of action and role in cancer prognosis. Unlike LRIG1, LRIG2 has been shown to interact with its targets in a stimulatory fashion, increasing PDGFRβ signaling in glial cells with downstream increases in proliferation rate (164), and increasing EGFR signaling *in cis* as well as *in trans*, also through proteolytic shedding of the extracellular domain (165). Similar increases in receptor expression have also been observed when LRIG3 is overexpressed (166), and LRIG3 has been shown to form stabilizing heterodimers with ErbB family proteins, which indicates an opposing role compared to LRIG1, but the functional end result is complicated since LRIG3 itself is inhibited by LRIG1 (167). Dysfunction in either protein is linked to developmental defects. Mutations in *LRIG2* cause urofacial syndrome, a disease characterized by inverted facial expressions, bladder dystonia and muscle weakness, all due to dysregulated nerve axon guidance during development (168,169). *Lrig3* knockout mice run in circles due to vestibular dysfunction, caused by deficient regulation of *Netrin1* mediated formation of the lateral canals of the vestibular organ (166,170). As for their roles in cancer, LRIG2 is hypothesized to act as an oncogene, as high expression has been associated with worse clinical outcomes in cervical cancer (171) and oligodendroglioma (172), whereas *Lrig2*-deficient knockout mice developed fewer and lower grade gliomas in a PDGFRβ-driven gliomagenesis model (173). The effect of LRIG3 on clinical outcomes is less clear, but survival in oligodendroglioma has been linked to subcellular localization of LRIG3 (174), and the presence of LRIG3 in adenocarcinoma of the uterine cervix seems to be a positive prognostic factor (156).

LRIG proteins in non-small cell lung cancer

At the beginning of the present project, nothing was known about the biological role of LRIG proteins in NSCLC and whether or not LRIG1 proteins were of clinical importance in this disease. However, it could be hypothesized that LRIG family members could be of importance, given the biological importance of EGFR signaling in NSCLC that was mentioned earlier. Furthermore, a study by Boelens *et al.* (175) showed that *LRIG1* is one of the genes in normal airway epithelium that is significantly downregulated by smoking, and that *LRIG1* is further downregulated after progression to lung squamous cell carcinoma. Our goal was therefore to investigate the prognostic and biological roles of LRIG proteins in NSCLC.

Aims

The overall aim of this project was to determine the prognostic and biological roles of LRIG proteins in NSCLC. Specifically, our aims were to:

- Investigate whether LRIG proteins are of prognostic importance in surgically treated NSCLC.
- Investigate the regulation of LRIG proteins themselves, by identifying and studying novel interaction partners and determining their role in NSCLC.
- Investigate possible biological mechanisms for LRIG proteins in lung cancer.

Materials and methods

Tissue microarray and immunohistochemical staining

A tissue microarray (TMA) containing samples from a clinical cohort of 355 surgically treated early-stage NSCLC patients, as described earlier by Botling *et al.* (176), had been assembled with two representative cores per patient, 1.0 mm in diameter, with a set of 17 histologically normal controls obtained from the same surgical specimens. All studies on the clinical cohort were carried out in accordance with the Code of Ethics of the World Medical Association (the Helsinki declaration) and with the approval of Uppsala university board of ethics, reference #2006/325. A corresponding database was established describing age, sex, smoking status, clinical stage, histological subtype, performance status at diagnosis, and survival time. Eight cases were excluded due to absence of assessable tissue in the sectioned and stained slides. A statistical overview of the 347 cases included in the present studies is provided in Table 4.

The TMA blocks were cut into 4 µm sections and stained in an automated fashion using a Ventana system (Ventana, Tucson, AZ, USA). Primary antibodies were produced by AgriSera, Vännäs, Sweden. Polyclonal rabbit antibodies against human LRIG1, LRIG2 and LRIG3 were previously described in (174,177,178). Polyclonal antibodies against human LMO7 were generated by immunizing rabbits with the synthetic peptide CTQSPTPRSHSPSAS (LMO7-1250). Resulting antisera were affinity purified using the corresponding peptide linked to UltraLink columns (Pierce Chemical, Rockford, IL, USA). For the immunostainings, all TMA sections were incubated with 6 ng/ml of antibody and horseradish peroxidase-linked goat anti-rabbit secondary antibodies, then counterstained using eosin. Samples were assessed independently by two investigators under supervision by an experienced lung pathologist. For each stain, staining intensity was graded on a scale from 0 to 3 (examples, using LRIG1 and LMO7 stains, shown in Figure 5) and the percentage of positive tumor cells was rounded to the nearest multiple of 25%. A staining score was then calculated by multiplying the staining intensity with the percentage of positive cells. For LRIG1, a separate assessment using the same scoring system was also performed on stromal cells.

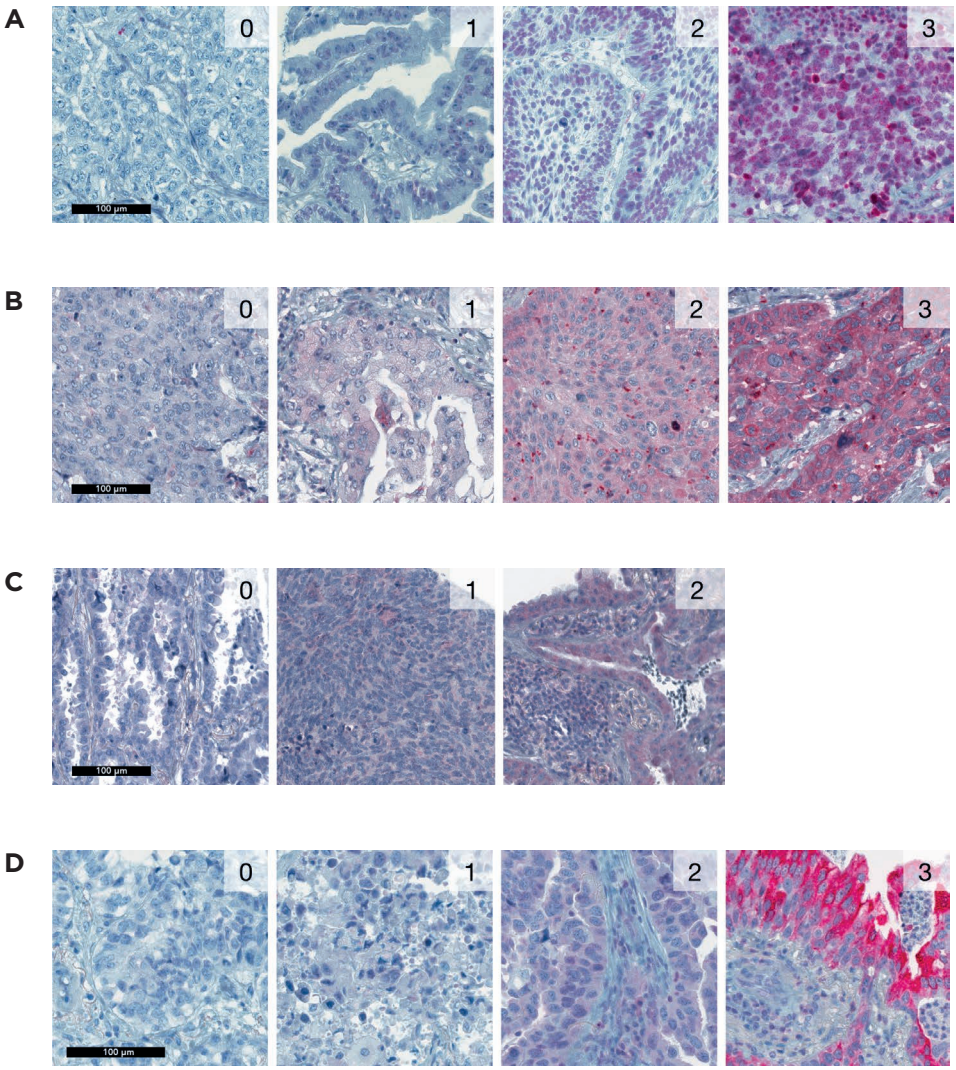

Figure 5. *Examples of stained TMA cores.* (**A**) Examples of LRIG1 stains. TMA sections were immunostained in a Ventana system using a polyclonal rabbit anti-LRIG1 antibody, then evaluated for staining intensity on a 0–3 scale. Shown are examples rated as intensities 0 through 3, left to right. Scale bar, 100 µm. (**B**) LRIG2 immunostains evaluated using the same 0–3 scale. (**C**) LRIG3 immunostains. No grade 3 stains were observed in the TMA cores. (**D**) LMO7 immunostains.

		Count	Percentage	Median
Sex	Female	162	46.7%	
	Male	185	53.3%	
Age				67
Smoking status	daily smoker for at least one year	162	46.7%	
	former smoker, non-smoker for >1 year	150	43.2%	
	never-smoker	33	9.5%	
Performance status	0	183	52.7%	
	1	131	37.8%	
	2	27	7.8%	
	3	5	1.4%	
	4	1	0.3%	
Histology	Squamous cell carcinoma	117	33.4%	
	Adenocarcinoma	191	55.0%	
	Large cell carcinoma	38	11.0%	
	Other	1	0.3%	
Stage	I	234	67.4%	
	II	53	15.3%	
	III	51	14.7%	
	IV	9	2.6%	

Table 4. Patient characteristics of the 347 cases in the cohort represented in the tissue microarray.

In silico and quantitative RT-PCR gene expression analyses

Publicly available datasets providing *LRIG1* mRNA expression data from surgically obtained whole tumor lysates, along with patient age, sex, smoking status, clinical stage and histological subtype, was analyzed using version 4.4.3 of the Oncomine browser (Compendia Bioscience, Ann Arbor, MI, USA). All lung cancer studies providing more than 100 cases were retrieved and included in our analysis. Univariable and multivariable survival analyses were performed, comparing the level of *LRIG1* mRNA expression with clinical outcome.

Tissue specific expression levels of *LMO7* and *LIMCH1* mRNA was measured in total RNA samples obtained from the following suppliers: small intestine, testicle, thymus, stomach, colon and spleen (Thermo Fisher, Waltham, MA, USA); kidney, placenta, heart, liver, and brain (BD Biosciences, San Jose, CA, USA); thyroid and lung (Agilent, Santa Clara, CA, USA). Quantitative reverse transcriptase PCR (qRT-PCR) was performed with the following primer/probe sets; *LMO7*: Hs01009229_m1 (Thermo Fisher); *LIMCH1*: Hs00971627_m1 (Thermo Fisher) and *RN18S* (18S ribosomal RNA) as previously described (177), using the ThermoScript™ RT-PCR System (Thermo Fisher) as previously described (177). Standard curves for *LMO7* and *LIMCH1* were prepared using *in vitro* transcribed RNA and the standard curve for *RN18S* was prepared using lysates from HEL2 cells. Expression levels of *LMO7* and *LIMCH1* were normalized against *RN18S.* All experiments were performed in triplicates.

An *in silico* analysis of *LMO7* and *LIMCH1* expression in normal tissues was performed on datasets in the Human Protein Atlas (HPA) (179), available at proteinatlas.org. The expression levels of *LMO7* and *LIMCH1* in NSCLC were analyzed in datasets from the cancer genome atlas (TCGA) using the USCC Cancer Genomics Browser (180), with comparisons of the expression levels in 533 adenocarcinomas, 502 squamous cell carcinomas and 108 tumor-adjacent normal tissues.

Statistical methods and survival analysis

Statistical analyses were performed using either SPSS (IBM, Armonk, NY, USA) or Jamovi (181,182) statistical packages. Tests for statistical significances between two normally distributed datasets were performed using independent values Student's *t*-test and comparisons with single normally distributed datasets against numeric constants using single values *t*-test. For datasets not exhibiting normal distribution, non-parametric hypothesis testing was performed using Mann-Whitney *U*-tests. Datasets with multiple linked measurements were analyzed using repeated measures ANOVA or, in case of non-parametric data, Wilcoxon's signed rank test.

For our survival analyses, appropriately sized groups were defined according to IHC scores by either setting a cut-off at the median, comparing negative cases against positive cases, or a combined approach treating negative cases as one group and splitting the positive cases at the median into a high and

low expressing group. Univariable survival analysis was performed by plotting cases in both groups by survival time in a Kaplan-Meier curve and testing for significance using log-rank tests. For multivariable analysis, the factor of interest (LRIG1, LRIG2, LRIG3 or LMO7) was added to a Cox proportional hazards model with binary covariates age (over or under median), sex, performance status at diagnosis (0–1 compared to ≥ 2), histological subtype (adenocarcinoma or SCC) and clinical stage (Ia compared to Ib–IIb).

Generation of plasmids and lentiviral particles

Doxycycline inducible LRIG1 overexpression vectors, as well as bicistronic lentiviral FLAG-tagged stable LRIG1 overexpression vectors carrying either red *mCherry* or green *ZsGreen1* fluorescent reporter genes, were generated by first amplifying a human *LRIG1* cDNA (Gene bank accession no. AF381545) using a CloneAmp HiFi PCR kit (Takara Bio, Kyoto, Japan) with primers with 15 bp complementarity 5' and 3' to the intended insertion site in a p3XFLAG-CMV-13 vector (Sigma-Aldrich, St. Louis, MO, USA). The vector was linearized using FastDigest HindIII and EcoRV restriction enzymes (Fermentas, Stockholm, Sweden), run on an agarose gel, excised using an E.Z.N.A. gel extraction kit and co-incubated in an In-Fusion EcoDry reaction (Takara Bio), in which a seamless Golden Gate type assembly is performed with a 2:1 molar ratio between the insert and target vector. Alignment and insertion were verified using restriction analysis. From this intermediary vector, a complete linear *LRIG1* insert with an upstream preprotrypsin leader and a C-terminal FLAG tag was further amplified using primers complementary to the intended insertion site at the multiple cloning site (MCS) region in the final pLVX-IRES-mCherry and pLVX-IRES-ZsGreen target vectors. Vectors were linearized using restriction enzymes NdeI and BamHI (Fermentas), purified by gel extraction and incubated in an InFusion reaction with the FLAG-tagged inserts (Figure 6). Resulting plasmids pLVX-LRIG1-IRES-mCherry and pLVX-LRIG1-IRES-ZsGreen1 were restriction analyzed to verify proper insertion and then sequenced to verify directionality and absence of point mutations.

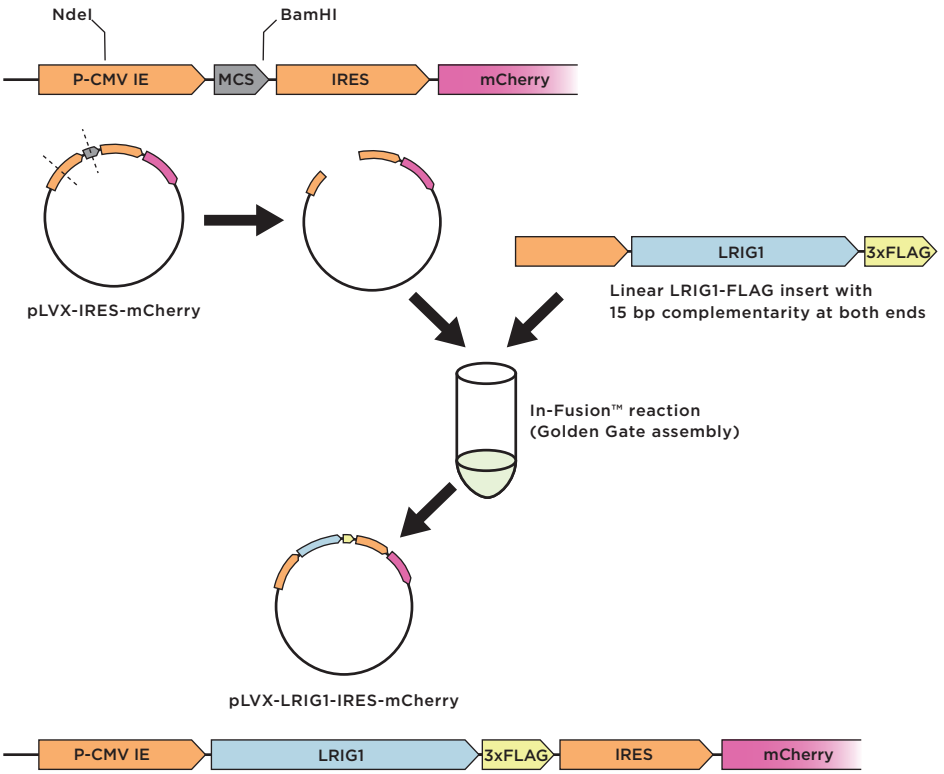

Figure 6. *Assembly of bicistronic LRIG1 overexpression vectors.* LRIG1 cDNA was tagged with a FLAG sequence at the 5' end and inserted at the 3' end of the internal ribosomal entry sites of the bicistronic pLVX-IRES-mCherry and -ZsGreen1 vectors. The final vectors code for mRNAs that are translated to two separate proteins, LRIG1 and a fluorescent reporter.

In a similar fashion, LMO7 and LIMCH1 vectors were generated by amplifying cDNAs from a Marathon lung cDNA library (Takara Bio) and inserted into a TOPO4 vector (Thermo Fisher, Waltham, MA, USA), after which the final inserts were amplified and sub-cloned into mammalian vectors pMH and pcDNA3.1 that had been linearized using the KpnI restriction enzyme. Correct sequence, directionality and insertion point was verified using restriction analysis and sequencing.

Cell culture and reagents

For mechanistic experiments in the included studies, human primary lung cancer cell lines A549, H1299, H1975, H460, H520 HCC827 (ATCC, Manassas, VA, USA) were used along with immortalized non-malignant cell lines Lenti-X HEK293T (Takara Bio) and COS-7 (ATCC). Lung cancer cells were cultured in RPMI-1640 medium (Sigma-Aldrich) with 10% fetal bovine serum (FBS) and 1 μg/ml of gentamicin (Thermo Fisher). HEK293 and COS-7 cells were cultured in DMEM medium (Sigma-Aldrich) with 10% FBS and 1 μg/ml of gentamicin. Cell lines were verified to be pathogen-free at IDEXX BioAnalytics (Ludwigsburg, Germany).

Lentiviral transductions and transient transfections

For the pLVX-LRIG1-IRES-mCherry and pLVX-LRIG1-IRES-ZsGreen1 vectors, as well as the pLVX-LRIG1-TRE3G vector previously described in (183), lentiviral particles were generated by transiently transfecting Lenti-X HEK293T cells according to the manufacturer's instruction, incubating for 24 hours and harvesting supernatants of culture medium that were filtrated using a 5 μm filter to remove cells. Viral supernatants were used directly or kept at −80°C.

For lentiviral transductions, primary lung cancer cell lines were seeded into 24-well plates and grown to approximately 80% confluency. For each well, the cell culture medium was replaced by 700 μl of fresh medium containing 1 μl of 6 mg/ml polybrene solution (Sigma-Aldrich). 300 μl of viral supernatant was added, and plates were centrifuged at 240 × *g* for 90 minutes. Cells transduced with fluorescent reporters were selected by their corresponding excitation/emission wavelengths through fluorescence-activated cell sorting (FACS) in a FACSAria III machine (BD Biosciences, East Rutherford, NJ, USA). TRE3G vectors were selected by adding 1 μg/ml of puromycin (Sigma-Aldrich) and 1 mg/ml of G418 (ThermoFisher) to the cell culture medium. All transduced cell lines were authenticated with regard to their original parental cell lines through short tandem repeat profiling via IDEXX BioAnalytics.

Transient transfections were performed on HEK293 cells and COS-7 cells using X-tremeGENE 9 (Roche, Basel, Switzerland) co-incubated in serum free media with LMO7-pcDNA3.1 or LIMCH1-pcDNA3.1 plasmids, according to the manufacturer's instructions, then incubating the cells for 48 hours before fixation or lysis.

Yeast two-hybrid screening

A yeast two-hybrid (YTH) screen was carried out by Dualsystems AG (Zürich, Switzerland) using a bait fragment known to be conserved across LRIG proteins, that was generated by subcloning cDNA encoding amino acids 831 through 881 of LRIG3 into the vector *pLexA-DIR* (Dualsystems AG), The bait construct was transformed into the strain DSY-1 (MATa his3Δ200 trp1-901 leu2-3,112 ade2 LYS2::(lexAop)4-HIS3 URA3:: (lexAop)8-lacZ GAL4) as described by Gietz *et al.* (184). Verification of bait expression was performed using western blotting using a mouse monoclonal antibody against the LexA protein as probe (Santa Cruz Biotechnology, Santa Cruz, CA, USA). To test for self-activation, DSY-1 yeast cells were transformed with the bait plasmid along with a negative control prey and grown in selective medium lacking the amino acids tryptophan, leucine, and histidine. The final YTH screen was performed by co-transforming DSY-1 with the bait together with preys from a human brain cDNA library. Two hundred transformants were screened. Positive transformants growing on selective medium were further tested for β-galactosidase activity using a filter assay (185) and transformants lacking β-galactosidase activity were discarded as false positives. Library plasmids were isolated from positive clones and screened in a bait dependency test using the bait plasmid and a negative control bait encoding a LexA–LaminC fusion using a mating strategy (186). Positives showing β-galactosidase activity when co-expressed with the bait but not with the control bait were considered bait-dependent positive interactors. The identity of positive interactors was determined by nucleotide sequencing.

Western blotting and co-immunoprecipitation

Cells were first cultured to approximately 90% confluency in either 6-well plates or 30 mm petri dishes (Sarstedt, Nümbrecht, Germany). Lysis buffers used were buffer B (1% Triton X-100, 9 mM NaCl, 3 mM Tris) for western blotting and Dynabeads IP buffer (ThermoFisher) for co-immunoprecipitation experiments, both with EDTA-free Complete protease inhibitor cocktail (Roche) added. Cells were washed once in 1x phosphate buffered saline (PBS), then lysed on ice in 200 µl of lysis buffer for 30 minutes. Nuclei were pelleted by centrifuging at 20,000 × *g* for 10 minutes and supernatants containing cytosolic proteins were transferred to new tubes. Concentrations were measured using the bicinchoninic acid (BCA) assay (187) and samples were kept at −20°C prior to use.

Western blotting was performed by thawing lysates at 4°C, then adding 4x LDS buffer and 10x sample reducing agent (ThermoFisher) followed by denaturing at 70°C for 10 minutes. Denatured samples were added to the wells in pre-cast 3–8% Tris-acetate gradient gel cassettes (ThermoFisher), and electrophoresis was performed at 160 V for approximately 45 minutes. Proteins were transferred onto low fluorescence polyvinylidene fluoride membranes using a semidry transfer method in a TurboTransfer machine (Bio-Rad). Membranes were blocked in Odyssey blocking buffer (Li-Cor, Lincoln, NE, USA). Primary antibodies used were mouse anti-FLAG M2 (Sigma-Aldrich), 1:2000, rabbit anti-LRIG1 (AgriSera), 1:1000, rabbit anti-LRIG3 (AgriSera), 1:1000, rabbit anti-LMO7 (AgriSera), 1:1000, rabbit anti-actin (Sigma-Aldrich), 1:5000 and mouse anti-actin (Abcam, Cambridge, UK). Secondary antibodies used were IRDye goat anti-rabbit 680 nm, 1:15,000, and IRDye goat anti-mouse 800 nm, 1:15,000 (Li-Cor). Membranes were fluorescently scanned at 700 and 800 nm using an Odyssey scanner (Li-Cor) at 164 or 84 µm resolution.

Co-immunoprecipitation was performed on lysates from COS-7 cells co-transfected to ectopically express LRIG1 along with either LMO7 or LIMCH1. Polyclonal rabbit antibodies against LRIG1 and LMO7 were coupled to magnetic protein A-coated microspheres (Dynabeads, ThermoFisher) using 10 µg antibody per mg of beads. Beads were washed and resuspended, then co-incubated with lysates on a rotator at 10 rpm for 1 hour in 4°C. Supernatants were transferred to separate tubes. Precipitates with beads and bound proteins were washed and resuspended in IP buffer. Western blotting, as described above, was then performed using both supernatants and precipitates.

Immunofluorescence and co-localization assays

Immunofluorescent imaging on cultured cells was performed on COS-7 cells seeded onto no. 1.5 cover slips (Zeiss) that were co-transfected with FLAG-tagged LRIG1 or LRIG3 (vectors LRIG1-pcDNA3.1 and LRIG3-pcDNA3.1, respectively), together with Myc-tagged LMO7 or LIMCH1 (vectors pMH-LMO7-Myc and pMH-LIMCH1-Myc) and incubated for 48 hours, then fixed using 4% paraformaldehyde. Cells were permeabilized and blocked in PBS containing 5% FBS and 0.05% Tween-20. Cells were labeled with primary antibodies, mouse anti-Myc (#ab32, Abcam) and rabbit anti-FLAG M2 (#2368, Cell Signaling, Danvers, MA, USA), and incubated for 1 hour followed by repeated washes in PBS. Labeled cells were then incubated with species appropriate fluorescent conjugated secondary antibodies, Alexa Fluor 488 and Alexa Fluor 555 (Life Technologies, Carlsbad, CA, USA) in the same fashion. Nuclei were counterstained and samples were mounted using Prolong Gold with 4,6-diamidino-2-phenylindole (DAPI) (Life Technologies).

Formalin fixated and paraffin embedded tissue sections were sectioned into 4 μm sections and placed on glass slides, rehydrated and blocked using tris buffered saline with 0.05% Tween-20 (TTBS) and 5% FBS. Sections were subsequently labeled using primary antibodies, mouse anti-mCherry and rabbit anti-ZsGreen (Takara Bio) diluted in blocking solution and incubated for 1 hour followed by repeated washes in TTBS. Sections were then labeled using species appropriate Alexa Fluor 488 and 555 antibodies in the same fashion as labeled cells.

Imaging was performed on a Zeiss LSM 710 confocal microscope equipped with Plan APO 63x 1.4 NA objective lens controlled by Zeiss ZEN software. Pixel size was set according to the Nyquist criterion and Z stacks with 0.6 μm thickness were acquired. To quantify co-localization in stained co-transfected cells, images were pre-processed and cellular regions of interest (ROIs) were manually segmented using ImageJ (188). The cellular ROIs were used to quantify the Pearson coefficients using the JACoP plugin.

Proximity ligation assay

To visualize and quantify protein-protein interactions at endogenous levels, proximity ligation assay (PLA) was performed using the Duolink II kit (Olink, Uppsala, Sweden) using the previously mentioned polyclonal LRIG1 and LRIG3 antibodies in conjunction with LMO7-1250 or rabbit isotype control antibodies. The H460 cell line was selected for this assay since it expresses detectable endogenous levels of LMO7 as well as LRIG1 and LRIG3 (data not shown). Cells were seeded onto no 1.5 coverslips (Zeiss) with or without transfection using LMO7 small interfering RNA (siRNA, #149889, Thermo Fisher), with non-targeting siRNA (Thermo Fisher) as negative control. PLA reactions were carried out according to the manufacturer's instructions and the generated circular DNA, indicating a physical interaction, was fluorescently labeled. Cells were mounted using mounting medium with DAPI (Life Technologies) and scanned using an LSM 710 confocal microscope using a Plan Apo 63x 1.4 NA objective lens at 12 bit into a 1024 × 1024 image. Z stack thickness was set according to the Nyquist theorem.

For quantification, Z stacks were imported into ImageJ (188). PLA spots and nuclei were detected using the 3D Objects Counter plugin and the number of PLA spots per cell was determined by assigning each spot to the nearest nucleus based on the Euclidean distance.

Animal strains and husbandry

For the *in vivo* experiments, female CIEA NOG mice (NOD.Cg-*Prkdc*^{scid} *Il2rg*^{tm1Sug}/JicTac, Taconic, Ejby, Denmark) lacking mature B, T and NK cells were obtained and kept at the animal facility at Umeå Centre for Comparative Biology. Animals were kept in individually ventilated cages, max 4 per cage, at a regulated temperature with a 12-hour day/night cycle. Mice were fed standard chow and water *ad libitum* and cages were equipped with standard enrichments to allow for normal behavior.

Ethical considerations

Translational studies involving the TMA cohort were carried out in accordance with The Code of Ethics of the World Medical Association (Declaration of Helsinki) and approved by the Uppsala regional ethical review board (reference #2006/325). Patient data were anonymized with a database key that was physically kept at the lab and never uploaded to any online services.

The animal experiments in this research project were kept at a minimum by using *in vitro* procedures whenever possible, and by designing the experiments to require as few animals as possible. The animal experiments in the present study were approved by the animal ethics board at Umeå university (dnr A 28-15). All experiments were performed under general anesthesia and the mice were given intraperitoneal buprenorphin and/or paracetamol supplemented drinking water after potentially painful procedures. Mice were observed daily for symptoms and euthanized under general anesthesia at the first sign of symptoms.

Orthotopic implantation

A pilot study was performed to determine the metastatic potential of four NSCLC cell lines. A549, H1299, H1975 and HCC827 cells were cultured to near confluency and then resuspended at either 1×10^6 or 1×10^7 cells per ml in 60 µl aliquots fresh RPMI medium supplemented with 20% purified matrix proteins (Geltrex, Life Technologies), then kept on ice until implantation. Mice were anesthetized and a 50 µl volume of cell suspension, corresponding to 50,000 or 500,000 cells, was injected using an ultrasound guided stereotaxic apparatus through the 7th or 8th dorsal intercostal space to a depth of 3 mm into the parenchyma of the left lung. Animals were observed until development of symptoms or after a maximum interval of 10 weeks, then euthanized. Liver, lungs, brains and all organs with macroscopically visible metastases were fixated in 4% paraformaldehyde solution, paraffin embedded, sectioned and stained using hematoxylin/eosin.

For the final experiment, stably transduced fluorescently labeled H1299 cells were pooled with a 50:50 mixture of either $H1299^{LRIG1\text{-}mCherry}$ and $H1299^{control\text{-}ZsGreen}$ for half the mice, or $H1299^{LRIG1\text{-}ZsGreen}$ and $H1299^{control\text{-}mCherry}$ for the other half. Pooled cells were resuspended in the same way and a volume of 50 µl containing 500,000 cells were injected in the left lung using the same method as in the pilot study. After euthanization, livers and both lungs were

removed. The superior lobe of the right lung, half the single lobe of the left lung and samples of liver metastases were alcohol. Purified DNA was extracted from the middle and postcaval lung lobes, the other half of the left lung and representative samples of liver metastases using a blood and tissue DNA kit (Qiagen, Germantown, ND, USA).

Magnetic resonance imaging

Magnetic resonance imaging (MRI) was performed on live tumor bearing mice using a 9.4 T Bruker Biospec 94/20 USR micro MRI (Bruker, Billerica, MA, USA). Mice were put under general anesthesia using 3.5% isoflurane in pure oxygen, with a 2% maintenance dose during procedures. Body temperature was monitored using a rectal probe thermometer and kept as close to 37°C as possible using circulating water in a heating pad. A pressure pad type sensor was used to monitor respiration frequency and breathing pattern. Respiration gated T1 FLASH sequences were acquired using the following parameters: TR = 113 ms, TE = 2.8 ms, flip angle = 30 degrees, field of view = 30 mm, matrix = 256 × 256 and 16 averages. 15 axial slices were obtained with 0.50 mm slice thickness and 1.00 mm interslice spacing. More axial slices were added as needed in order to cover the lungs in their entirety on larger mice. A 40 mm quadrupolar volume coil was used in transmit/receive mode.

Digital droplet PCR

Digital droplet PCR (ddPCR) was used for detection and copy number quantification of gene segments. In our ddPCR assays, purified genomic DNA was pre-digested using sequence appropriate enzymes (FastDigest NdeI and BamHI, Fermentas) at 37°C for 15 minutes, then heat inactivated at 70°C for 5 minutes. Reaction mixtures were prepared according to the manufacturer's specifications using dUTP-free reagent mixture for probes (BioRad), primers for our genes of interest at a concentration of 900 nM and double quenched FAM or HEX probes at a concentration of 250 nM. Nanoliter-sized droplets were generated into droplet oil using a QX100 droplet generator (Bio-Rad) and pipetted onto 96-well PCR plates which were foil sealed. Each plate was run for 10 min at 95°C followed by 40 cycles of 95°C for 30 sec and 56°C for 60 sec, then a final step at 98°C for 10 min, then analyzed in a ddPCR droplet analyzer (Bio-Rad)

with automatic identification of positive droplets in the FAM and HEX channels if possible, otherwise manual thresholding at a signal amplitude of 1,500. For samples representing mixed populations harboring LRIG1 overexpression vectors and empty control vectors, a ratio was calculated between the copy numbers of each vector.

Transwell and wound closure assays

Cell migration was performed using a transwell assay (189) by serum starving cells at approximately 80% confluence in standard RPMI medium with 1% FBS for 24 hours, then detached using trypsin and counted in triplicates. Transwell inserts with polyethylene terephtalate plastic membranes and 4 μm pore size were placed into corresponding 24-well cell culture plates (Sarstedt). Cell suspensions were diluted using RPMI with 1% added FBS, to a concentration of 50,000 cells per ml. Inserts were filled with 100 μl of diluted cell suspension and the outer wells were filled with 600 μl of RPMI with 10% FBS. Plates with inserts were placed in a cell culture incubator for 24 hours. Non-migrated cells were removed from the insert chambers using a wet cotton swab. Inserts with attached migrated cells were subsequently methanol fixated at −20°C for 10 minutes, then stained using Meyer's hematoxylin solution. Migrated cells were manually counted using light microscopy, in a blinded fashion.

For our wound closure assay, cells were transferred to 6-well cell culture plates (Sarstedt) at a concentration of 100,000 cells per well. Plates were incubated for 24 hours to allow for proper attachment. Cross-shaped wounds were created in the cell monolayer in each well using a yellow 5–200 μl pipette tip. Detached cells were removed by washing wells twice in PBS. Fresh culture medium was added. Phase contrast images were obtained using an Axio Vert A1 microscope (Zeiss) immediately after washing. Plates were then placed in a cell culture incubator and images were obtained at regular intervals until wounds were closed. Quantification was performed in an automated double blinded fashion by measuring the wound area, using an ImageJ script performing edge detection with radius = 10 px, gaussian blur with radius = 5 px and Otsu thresholding. Wound closure time was subsequently calculated by comparing wound area for each well at all time points.

Live-cell imaging assays

A HoloMonitor M4 holographic microscope (Phase Holographic, Lund, Sweden) installed into a standard cell culture incubator was used to acquire live cell imaging data on cell motility and proliferation rate. Cells were seeded sparsely onto standard 6 well plates or 24-well Lumox plates (Sarstedt). 3 or 0.6 ml of culture medium, respectively, was added to each well, and the wells were then covered with clear plastic polymethyl methacrylate lids (HoloLids, Phase Holographic). Plates were placed in the HoloMonitor microscope and, using HoloMonitor software, eight or sixteen 0.52 × 0.52 mm imaging regions were determined for each well. All regions were continuously imaged at 8-minute time intervals for 48 or 72 hours. The built-in proliferation and population-based motility analysis modules in the HoloMonitor software were used to determine the average doubling times and migration speeds, in hours and μm/hour for each cell line.

Radiosensitivity and clonogenicity assays

Radiosensitivity was assessed using an early plating clonogenic assay, using Franken's modified version of the assay described by Puck and Marcus (190,191). Cells were plated onto 6-well culture plates (Sarstedt) with 250,000 cells per well, then incubated overnight. Irradiation was performed using a Clinac XI linear accelerator (Varian Medical Systems, Palo Alto, CA, USA). Each plate was placed in the gantry and wells were filled to the brim with standard culture medium to avoid air gaps, with perspex bolus plates on all sides as well as on top. Plates were irradiated with either 0, 1, 2, 4, 6, 8 or 10 Gy as a single dose. Within four hours of irradiation, cells were detached, counted and diluted in fresh medium to pre-determined concentrations. For each cell line and each radiation dose, cells were plated in triplicates onto six-well plates at a density of 300 cells per cm^2, then incubated until macroscopically visible colonies had formed. Plates with colonies were then fixated using methanol at −20°C for 10 minutes, stained using 0.05% crystal violet solution, washed twice in deionized water and dried.

The baseline clonogenic ability of each NSCLC cell line in our panel was determined in a similar fashion, but with plating of untreated cells in triplicates at a density of 100 cells per cm^2. In both assays, the number of stained colonies was quantified in an automated and blinded fashion. Grayscale images of plates

with stained colonies were captured using a ChemiDoc XRS imager (Bio-Rad) with a white light conversion screen, with the same exposure time, black point, white point and gamma setting for all images, and with a corresponding empty image for each capture session. Images were imported into ImageJ and processed using an automated script, first normalizing background levels by subtracting the corresponding empty image, then performing binary thresholding (level = 10), noise removal using sequential max and min filtering (radius = 1 px) and watershed filtering. Colonies were counted using the object counter plugin, on a per well basis using circular ROIs.

Dose response and cell proliferation assays

For our dose response assays, biological duplicates of all transduced fluorescent variants of H1299 and H1975 cells (LRIG1 or empty vector, coupled to mCherry or ZsGreen as described earlier) were seeded onto entire rows of multiple 96-well plates (Sarstedt) at a concentration of 10,000 cells per well and incubated for 24 hours. Aliquots of culture medium with a linear dilution of drugs, at a dose span corresponding to levels expected in human tissues during treatment, were prepared by diluting cisplatin or vinorelbine (Sigma-Aldrich) in fresh culture medium. For cisplatin, concentrations from 0 to 100 µmol/l in steps of 10 were prepared. For vinorelbine, concentrations of 0 to 1,560 nmol/l were prepared in steps of 60. The culture medium on the 96-well plates was replaced with drug containing medium, with triplicate wells for each cell line variant and drug concentration. Plates were incubated for 48 and 72 hours.

To determine cell viability and proliferation rate, the resazurin reduction assay was used (192). 20 µl of 0.15 mg/ml resazurin solution was added to each well and plates were incubated for 4 hours, then scanned using a SpectraMax i3 spectrophotometer (Molecular Devices, San Jose, CA, USA) set to excitation = 530 nm and emission = 590 nm. This was performed on one set of plates immediately after plating, on another set at treatment start and then after 48 and 72 hours of treatment. Dose response was assessed both by calculating IC_{50} values using logarithmic regression, and in a time-invariant fashion as described by Hafner *et al.* (193) by first establishing a growth curve for each cell line, then calculating a treatment-dependent and time-independent growth rate, GR(c), by comparing the slope of the viability signal against that of untreated controls, for each treatment.

Results and discussion

LRIG1 was a positive prognostic marker for survival in early-stage NSCLC (I)

In our cohort of 347 surgically treated, early-stage NSCLC patients, we found that the amount of cases with a completely negative LRIG1 immunostain was close to half the entire cohort, placing the median immunoreactivity score at only 0.15, which would have been an impractical cut-off value to determine dose-response effects. In order to determine if there were differences in survival between patients with high and low IHC scores, we chose to treat the negatives as a separate group and then split the positive cases at the median (score 0.66), creating three groups: one with score 0, and two equally sized groups with scores 0.01–0.66 (low LRIG1) and 0.67–3.00 (high LRIG1).

When comparing survival in the three groups, the group with a low score did not differ significantly from the negative cases. However, the group with high LRIG1 had a large and significant survival benefit of 33.2 months when compared to negative cases (Wilcoxon log-rank test, $p = 0.012$). When stratifying by histological subtype, a survival benefit was only observed for adenocarcinoma cases ($p = 0.014$). A stratification based on clinical stage showed that the survival benefit was limited to stages Ib, IIa and IIb ($p = 0.002$) but not stage Ia, III or IV. When compensating for already established prognostic factors in NSCLC, such as age, sex and WHO performance status, in a multivariable Cox regression analysis, the association between high LRIG1 and better survival remained significant, meaning that LRIG1 is an independent positive prognostic factor in NSCLC (Table 5). A similar comparison was performed across groups based on LRIG2 and LRIG3 immunoreactivity, but no differences in survival were observed.

To further test our hypothesis that high LRIG1 levels are associated with better clinical outcomes, we did an *in silico* analysis on mRNA expression data from large clinical cohorts in the Oncomine database (194). In this analysis, high *LRIG1* messenger RNA (mRNA) expression was also significantly associated with better survival in lung adenocarcinoma ($p = 0.007$), but a survival benefit was observed for SCC cases as well ($p < 0.001$). Since the mRNA expression data is performed on whole tumor lysates, whereas our IHC analysis was specifically looking at the tumor epithelium, we did an additional non-selective assessment of staining intensities in the LRIG1 immunostained TMA, including

Table 5. Multivariable Cox regression analysis evaluating the risk of death (HR) across groups based on LRIG1 expression, with compensation for already established clinical prognostic factors in NSCLC.

	Sig.	HR (95% CI)
Neg. LRIG1	—	1.000
Low LRIG1	0.622	1.078 (0.800–1.451)
High LRIG1	0.004	0.623 (0.449–0.863)
Symptomatic (PS > 0)	0.000	1.711 (1.320–2.219)
Stage > I	0.000	1.669 (1.280–2.178)
Age > median	0.001	1.569 (1.200–2.050)
Sex: female	0.084	0.890 (0.780–1.016)
Adenocarcinoma	0.693	0.948 (0.726–1.237)

stromal cells and infiltrating immune cells as well. When stratifying for LRIG1 IHC score, we then observed a corresponding survival benefit for SCC cases as well, indicating that the known *in trans* effects of LRIG1 (149,150,195) may be of clinical relevance, or that a survival benefit somehow is conferred by stromal cells or infiltrating immune cells that are LRIG1 positive.

It is of clinical interest that the survival benefit from high LRIG1 in tumor tissue was observed only for stages Ib, IIa and IIb, since that represents the subgroup of NSCLC patients that is offered adjuvant chemotherapy after surgery, whereas stage Ia patients had no differences in survival. The aim of adjuvant treatment is to prevent disease recurrence, but no such benefits have been observed in stage Ia (12). Thus, we hypothesized that LRIG1 either affects the chemosensitivity in NSCLC or, alternatively, exerts an effect on intrinsic biological properties involved in disease recurrence and development of metastatic disease.

LRIG1 and LRIG3 interacted physically with LMO7 and LIMCH1 (II)

To search for proteins possibly interacting with LRIG family, we performed a yeast two-hybrid screen testing for physical interaction with a cytosolic peptide that is largely conserved among the mammalian LRIG proteins. This screen resulted in 25 matches; 11 corresponding to the paralogous proteins LIM domain only 7 (LMO7), 13 to the paralogous protein LIM domains and calponin homology protein 1 (LIMCH1) and one sequence of unknown significance on chromosome 5. For both LMO7 and LIMCH1, the bait-dependent positive interactors were fragments situated at the C-terminal end and encompassing a

LIM domain (Figure 7). Since there were multiple clones corresponding to the same molecular entities, the interaction was not likely to be random or non-specific. Furthermore, LIM domains are commonly involved in protein-protein interactions (196-198), which further strengthened our hypothesis that the interaction represented a true protein-protein interaction.

In order to determine whether a protein-protein interaction occurs between full-length LRIG proteins and LMO7 or LIMCH1, we co-immunoprecipitated lysates from cells that had been transiently transfected to co-express either FLAG-tagged LMO7 or LIMCH1 together with LRIG1 or LRIG3. We found that both LRIG proteins co-precipitated with LMO7 as well as LIMCH1. When LRIG1 was used as bait for co-immunoprecipitation in lysates containing LMO7 or LIMCH1, a 160 kDa FLAG-reactive band corresponding to LMO7 (here referred to as LMO7 A), and a 154 kDa band corresponding to a major band of LIMCH1 (here referred to as LIMCH1 A) were detected in the precipitates. Two minor bands, referred to as LIMCH1 B and C, were absent in the LRIG1 precipitates. For LRIG3, LMO7 A was detected in the precipitates. In contrast to LRIG1, all three LIMCH1 species (bands A, B and C) co-precipitated with LRIG3.

To analyze the subcellular localizations of possible interactions, we performed an immunofluorescence analysis of cells transfected to co-express LRIG1 or LRIG3 together with LMO7 or LIMCH1 that showed significant co-localization for all four protein combinations. LMO7 expression was detected in the perinuclear area, along cytoskeletal-like structures and in the cytoplasmic periphery. LIMCH1 localized to the perinuclear area, cytoplasmic punctae and the cytoplasmic periphery. LRIG1 and LRIG3 localized to the perinuclear area, cytoplasmic punctae and the cytoplasmic periphery. Co-localization was observed for LRIG1 and LMO7 in the cytoplasmic periphery and at cytoskeletal-like structures in the cytoplasm (Pearson's coefficient = 0.621, SD ± 0.093, n = 9). LRIG1 and LIMCH1 co-localized in large cytoplasmic punctae and in the cytoplasmic periphery (Pearson's coefficient = 0.668, SD ± 0.065, n = 9). LRIG3 and LMO7 co-localized in the perinuclear region, in cytoplasmic punctae and at the edges of cells (Pearson's coefficient = 0.623, SD ± 0.028, n = 9). LRIG3 and LIMCH1 co-localized in the perinuclear region and at the edges of the cell (Pearson's coefficient = 0.581, SD ± 0.086, n = 5).

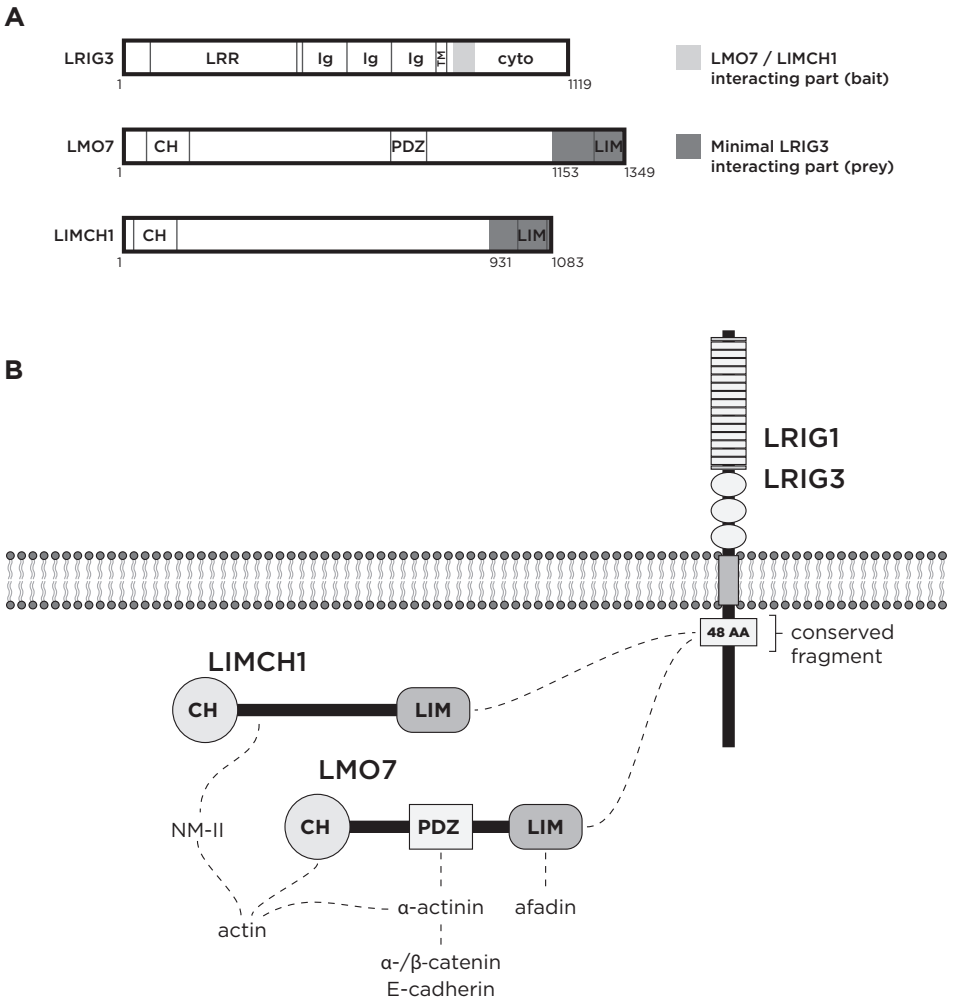

Figure 7. *LMO7 and LIMCH1 both interacted physically with LRIG1 and LRIG3.* (**A**) Yeast two hybrid screen. A fragment from the LRIG3 cytosolic domain, but present in all LRIG proteins, was used to screen for interacting peptides. The screen resulted in clones representing LMO7 and LIMCH1. Shown are schematics of the location of the interacting bait fragments. (**B**) Proposed interactions. The bait fragment represents a conserved 48 amino acid sequence that is present in both LRIG1 and LRIG3. LMO7 is known to interact with the E-cadherin/catenin system through its PDZ domain and has been predicted to bind actin through its CH domain. LIMCH1 has one other known interaction with nonmuscle myosin-II (NM-II). Adapted from (200-203).

We then proceeded with a proximity ligation assay (PLA) to see if protein-protein interactions also were taking place at endogenous levels. This assay uses two antibodies with coupled DNA strands, that cooperate in a rolling circle DNA amplification to create multiple labeled DNA loops at sites of interaction, visible as fluorescent spots, if the antibodies bind within the length of the coupled DNA strand (approximately 30 nm) of each other (199). The number of PLA spots was significantly higher when cells were labeled with antibodies against LRIG1 and LMO7 than with LRIG1 and isotype control (Student's *t*-test, $p < 0.0001$). The same was observed for LRIG3 and LMO7 ($p < 0.0001$). Furthermore, transient downregulation of LMO7 using siRNA transfection resulted in fewer spots for the LRIG1-LMO7 reaction ($p = 0.009$) and the LRIG3–LMO7 reaction ($p = 0.028$).

Thus, we had experimental evidence supporting that C-terminal regions of LMO7 and LIMCH1 physically interacted with a peptide motif present in all mammalian LRIG proteins, and evidence of physical interaction with LRIG1 and LRIG3 in a transient co-expression system showing physical interaction as well as subcellular co-localization when the proteins were ectopically overexpressed. The few LIMCH1 antibodies available at the time of our study proved unsuitable for PLA, but we could show that LMO7 is in extremely close proximity to LRIG1 and LRIG3 when expressed at endogenous levels, without resorting to overexpression systems. That means that we can say with high certainty that we have observed true protein-protein interactions that take place under normal conditions as well. Looking further, LMO7 is known to interact with the E-cadherin/catenin complex through its PDZ domain, also linking afadin to this complex through the LIM domain (200,201). It has been predicted to bind actin using its CH domain as well (202). The interactions of LIMCH1 are less studied, but the protein also interacts with the actin cytoskeleton by binding nonmuscle myosin-II using a coiled-coil motif near the N terminus (203). Thus, our findings add to the LRIG interactome (146) and implicate a role for LRIG proteins in cellular adhesion and migration.

The nature of the different molecular species of LMO7 and LIMCH1 observed in our assays is yet unknown. As with most muscle related genes, they both undergo a considerable degree of alternative splicing when expressed endogenously (204). Our western blots on ectopically overexpressed LMO7 and LIMCH1 proteins showed multiple FLAG-reactive bands at different molecular weights, but the overexpression vectors in that system are based on cDNA that is already spliced. This leads us to hypothesize that LMO7 and LIMCH1 undergo

post-translational modification as well. Since three LIMCH1 species co-precipitated with LRIG3, but only the largest one co-precipitated with LRIG1, the interaction with LRIG1 is either weaker or taking place at other sites in the cytosolic domain.

LMO7 and *LIMCH1* were downregulated in NSCLC and the prognostic value of LRIG1 expression was dependent on LMO7 status (II)

In order to investigate the expression levels of *LMO7* in normal human tissues, we measured *LMO7* and *LIMCH1* mRNA levels in commercially available tissue lysates and also did an *in silico* analysis of expression levels using datasets in the Human Protein Atlas (179). Using both methods, we found that lung tissue had the highest or second highest expression levels of both *LMO7* and *LIMCH1* of all tissues analyzed.

The findings on *LMO7* and *LIMCH1* expression in normal tissue made it of particular interest to determine whether changes in their expression could be observed in NSCLC. To investigate that, we performed an *in silico* analysis on datasets in the TCGA database. The expression levels of *LMO7* and *LIMCH1* were both significantly lower in NSCLC tumors compared to tumor-adjacent normal tissue. The differences were observed in adenocarcinomas (Student's *t*-test, $p < 0.001$) and squamous cell carcinomas ($p < 0.001$).

To further determine whether LMO7 levels in tumor tissue exhibit correlation with clinical outcomes in NSCLC, we immunostained the same TMA as previously stained for LRIG proteins for LMO7. We noted that a much larger proportion of cases were completely negative, as only approximately 30% of cores had a positive immunostain. Of these positive cores, only a select few had more than a weak immunostain, so we chose to compare the clinical outcome of negative cases with that of positive cases.

In our univariable survival analysis, we found that there was no significant correlation between LMO7 expression and patient survival. A multivariable Cox regression analysis showed no changes when the usual clinical risk factors (age, sex, clinical stage and performance status) were added as co-factors, as the risk of death was not significantly affected by LMO7 status. However, since we suspected an interaction between LRIG1 and LMO7, we added LRIG1 status as a co-factor in our Cox model, resulting in a significant LMO7-dependent

	Sig.	HR (95% CI)
LMO7 positive	0.013	1.416 (1.075-1.865)
LRIG1 negative	0.001	1.000
LRIG1 low	0.824	1.034 (0.769-1.392)
LRIG1 high	0.001	0.554 (0.394-0.779)
Symptomatic (PS > 0)	0.001	1.698 (1.314-2.194)
Stage > 1	0.000	1.657 (1.273-2.156)
Age > 70 years	0.001	1.565 (1.197-2.047)
Sex: female	0.096	0.805 (0.623-1.040)

Table 6. Multivariable Cox regression analysis evaluating the risk of death (HR) based on LMO7 expression, with correction for LRIG1 status as well as established clinical prognostic factors in NSCLC.

change in risk of death when compensating for clinical risk factors and LRIG1 status (Table 6). The latter is more easily comprehended when performing a univariable Kaplan-Meier analysis stratified for LRIG1 and then LMO7 status, since the only subgroup with a large and statistically significant survival benefit consists of cases with high LRIG1 level and a negative LMO7 immunostain. No survival benefit was observed for LRIG1 high cases positive for LMO7. Taken together with our *in vitro* findings of a direct protein-protein interaction, this provides strong clinical evidence that LMO7 physically interacts with LRIG1 in an inhibitory fashion.

One question that remains unanswered is whether or not a similar effect is seen for LIMCH1. LIMCH1 has been shown to inhibit the degradation of p53 protein in NSCLC cell lines (205) and has therefore been hypothesized to be a positive prognostic marker in lung adenocarcinoma. That suggests that the paralogs LMO7 and LIMCH1 might have somewhat opposing functions. However, at the time of our study, no commercial LIMCH1 antibodies were available and our in-house polyclonal LIMCH1 antibodies were not usable for IHC.

LRIG1 overexpression did not affect cell proliferation in most cell lines (III)

Since it could be a possible mechanism underlying the observed survival benefits associated with a high LRIG1 expression, we performed proliferation assays to investigate whether LRIG1 overexpression affects the cellular proliferation rate. This was performed using long-term live cell imaging on a panel of NSCLC cell lines transduced with inducible or stable LRIG1 overexpression vectors, with cellular proliferation rate expressed as population doubling time. When comparing $H1299^{LRIG1\text{-}mCherry}$ cells with $H1299^{control\text{-}mCherry}$ cells, the growth rate of the LRIG1 overexpressing population did not differ significantly from the vector control counterpart (Student's *t*-test, $p = 0.373$). For H1975, there was a possible trend towards slower proliferation when comparing $H1975^{LRIG\text{-}mCherry}$ with $H1975^{control\text{-}mCherry}$, but not significant ($p = 0.056$). H1299 and H1975 cell populations were also compared based on fluorescent reporter, but mCherry and ZsGreen1 had no effect by themselves on the proliferation rate in either cell line ($p = 0.227$ and $p = 0.547$, respectively).

In our panel of NSCLC cell lines with doxycycline inducible LRIG1 expression, the effects of LRIG1 overexpression on proliferation rates were similar. When comparing cells growing in doxycycline-containing medium with corresponding cells in control medium, proliferation rates did not differ at all for the A549 and H520 cell lines ($p = 0.875$ and $p = 0.267$, respectively). In a similar fashion as the stably transduced variant, H1975 cells with induced LRIG1 overexpression had a non-significant trend towards slower proliferation ($p = 0.057$). HCC827 was the only cell line with an effect of LRIG1 on proliferation, with a significant decrease observed for induced cells compared to controls ($p = 0.046$).

Thus, our conclusion from these experiments is that the observed survival differences of LRIG1 expression in NSCLC is not likely to be caused by a general effect on cancer cell proliferation rates. However, our findings do indicate that this might be a mechanism in NSCLC cases with tumor-driving *EGFR* mutations, since both HCC827 and H1975 are established from *EGFR* mutated lung adenocarcinomas. This would also be in line with previous knowledge that LRIG1 inhibits EGFR signaling (142,143). However, since our observed survival benefit affected a large proportion of cases, and was not associated with *EGFR* mutation status, it is unlikely that the observed effects on clinical outcome are due to slower tumor growth.

LRIG1 overexpression had inconsistent effects on migration but affected clonogenic ability (III)

Since we previously had observed that an LRIG1-dependent difference in survival was limited to the clinical stages in which adjuvant chemotherapy provides a survival benefit, and since the development of metastatic disease is the most common type of disease recurrence in NSCLC (206), we hypothesized that LRIG1 affects the metastatic potential of NSCLC cells. To investigate that, we performed a series of *in vitro* assays focused on invasion and migration, using the same panel of NSCLC cell lines as in the proliferation experiments.

To evaluate migration and invasion using well-established methods, we first performed a wound healing assay (also known as a scratch assay) and compared the effects of LRIG1 overexpression on H1299 and H1975 cells. For H1299, the LRIG1 overexpressing cells bridged the wound slightly but significantly faster compared to vector controls (Mann-Whitney *U*-test, $p = 0.029$). For H1975, no difference in wound closure rate was observed when comparing LRIG1 overexpressing cells with controls ($p = 0.857$). We then investigated chemotaxis and invasive potential on the same cell lines using the transwell assay (189). In this assay, we observed no difference in the number of migrated cells for either H1299 (Student's *t*-test, $p = 0.264$) or H1975 cells ($p = 0.356$).

One major issue with the wound healing assay is that it is difficult to determine to which degree the closure of a wound in a monolayer of cells is caused by migrating cells filling in the gap, or cell displacement due to proliferation. We therefore performed long-term live holographic imaging on cells growing under standard conditions, which allows for the cell migration to be measured directly and independently of proliferation rates. Imaging was performed on the stably transduced H1299 and H1975 cell lines, as well as the expanded NSCLC panel with inducible LRIG1 overexpression. Significant increases in motility rate were observed for LRIG1-overexpressing H1299, A549$^{\text{TetLRIG1}}$, H520$^{\text{TetLRIG1}}$ and HCC827$^{\text{TetLRIG1}}$ cells, while a significant decrease in motility rate was observed for LRIG1-overexpressing H1975$^{\text{TetLRIG1}}$ cells. However, the differences in motility rate were minor (Paper III, Figure 3A).

Another part of the metastatic process that can be modelled *in vitro* is clonogenic potential, which measures the proportion of cells capable of replicating and forming a viable colony of cells. This was assessed for the entire panel of NSCLC cell lines as well, using sparsely plated cells. We found significantly

decreased colony formation when LRIG1 was overexpressed in H1299, H1975 (both stably transduced and inducible cells) and HCC827 cells, and no differences in A549 and H520 cells (Paper III, Figure 2A). No cell line exhibited an increased colony forming ability when LRIG1 was overexpressed.

In summary, we observed minor and somewhat discordant effects on cell migration when LRIG1 was ectopically overexpressed. Results were largely similar in different assays, which reinforces our findings that LRIG1 does little to affect migration and invasion in NSCLC cell lines *in vitro*. However, the observed decrease in clonogenic potential is concordant across cell lines and might implicate that LRIG1-expressing circulating tumor cells have a decreased ability to form viable metastases in the metastatic niche.

Chemo- and radiosensitivity was unaffected by LRIG1 overexpression (III)

We had previously hypothesized that LRIG1 might affect tumor cell sensitivity to adjuvant treatments, and thus performed *in vitro* experiments assessing cellular chemosensitivity as well as radiosensitivity. Chemosensitivity was measured using cisplatin and vinorelbine, which are routinely used for adjuvant chemotherapy in NSCLC, at concentrations similar to those in human tissues during treatment (207-209). LRIG1 did not confer an increased sensitivity or resistance to cisplatin in either the H1299 or H1975 cell lines, with no significant effects on the IC_{50}. Both H1299 and H1975 cells turned out to be very sensitive to vinorelbine, with complete cytostasis at very low drug concentrations and no cytotoxicity at any tested concentration. Thus, IC_{50} could not be reliable calculated, but no significant differences in growth rate (GR) were observed at any concentration and there was no significant curve separation in a Wilcoxon test.

LRIG1 has previously been reported to increase the sensitivity to cisplatin in bladder cancer, gastric cancer and oesophageal carcinoma (210-212), at the same concentrations as was used in our study. However, judging from our results, the previously reported effects of LRIG1 on cisplatin sensitivity did not appear not to apply to the NSCLC cell lines. Effects of LRIG1 on vinorelbine sensitivity have only been reported in one study (212), in which considerably higher concentrations were required to see any biological effects. This means that H1975 and H1299 might already be inherently sensitive to vinorelbine.

Radiotherapy is not used in the adjuvant setting but is of clinical importance as more patients with localized disease are cured using SBRT or radiochemotherapy, rather than offered palliative treatment. We investigated the radiosensitivity of H1299 and H1975 cells using clinically relevant doses ranging from 0 to 10 Gy, followed by the standard colony forming assay (190,191). No differences in colony formation were observed when comparing LRIG1-overexpressing and vector control H1299 or H1975 cells at any fractional dose, indicating that LRIG1 did not significantly affect the radiosensitivity in these cell lines.

In summary, we did not observe any LRIG1-mediated effects on chemosensitivity, and thus conclude that the survival benefit observed in early-stage NSCLC cases is not due to increased sensitivity to adjuvant medical therapy. Furthermore, LRIG1 only confers minor changes on cellular radiosensitivity, which leads us to conclude that LRIG1 is unlikely to be suited as a predictive marker for either chemosensitivity or radiosensitivity.

LRIG1 was not significantly enriched in metastases compared to primary tumors (III)

Since *in vitro* studies only recapitulate single steps in the metastatic cascade, we wanted to recreate the entire metastatic process *in vivo* and investigate whether LRIG1 expression gives an advantage or disadvantage in the formation of metastases in immunodeficient mice. We first performed a pilot study using orthotopic implantation of non-transduced parental cells to determine the metastatic potential of each cell line. Briefly, H1299 was the only cell line forming hematogenously spread micrometastatic disease, with multiple cell clusters embedded in the alveolar walls of the contralateral lung. H1299 also formed overt macrometastatic disease with tumor growth in the in the pleura, mediastinal lymph nodes and liver. H1975 was somewhat metastatic but did not form any intraparenchymal micrometastases in the contralateral lung, only pleural metastases and lymph node metastases. HCC827, which represents a highly differentiated adenocarcinoma, only formed locally advanced disease with no visible symptoms.

In our final *in vivo* experiment, which accordingly was performed using H1299 cells, we formed mixed tumors by orthotopically injecting a population of fluorescently tagged LRIG1 overexpressing cells, pooled in a 1:1 fashion with vector control cells expressing a different fluorescent marker. We then analyzed

the ratio between the two gene vectors in the primary tumors and metastatic sites, as well as in saved samples from the injected cell suspension. The LRIG1-overexpressing population was enriched in the primary tumors compared to the injected suspension. However, the ratio of LRIG1 vectors to control vectors did not differ significantly between the primary tumors and the metastatic sites. This means that the only biological effect of LRIG1 we observed in this experiment was that LRIG1 somehow enhanced cell survival and establishment of a primary tumor during the process of orthotopic injection using the H1299 cell line, but that it had no effects on the formation of hematogenous metastases.

One major weakness in this study is that even though the metastatic process is recapitulated in its entirety in this model, it relies on a cell line representing advanced disease. Most, or all, of the available NSCLC cell lines have been established either from malignant pleural effusion or lymph node metastases. Biologically, that means that the cells already have acquired the ability to form metastases, which makes it difficult to draw conclusions on mechanisms in early-stage disease. Also, the surgical technique used in the curation of NSCLC involves prolonged tissue ischemia prior to removal of the tumor, which makes it impossible to establish cell lines from surgically removed early-stage primary tumors. In order to establish cell lines from early-stage disease, it might thus be necessary to use cells from computer tomography guided biopsies, which adds an ethical dilemma regarding patient risks. Regardless, to our knowledge, this is the first time ddPCR quantification has been used to quantify selection effects in metastasizing mixed-population tumors, and we believe the method in itself might be useful for answering other scientific questions on NSCLC metastases in the future.

Conclusions

High levels of LRIG1 in tumor tissue was associated with a large and significant survival benefit of 33.2 months, compared to negative cases, in a cohort of surgically treated early-stage NSCLC patients. Significant survival benefits were observed for patients with lung adenocarcinoma and clinical stages Ib, IIa and IIb. Based on our findings, LRIG1 is a candidate positive prognostic marker for surgically treated early-stage NSCLC.

The paralogous proteins LMO7 and LIMCH1 physically interacted with a conserved part of the cytosolic domains of LRIG1 and LRIG3. The protein-protein interaction had clinical implications, since the survival benefit conferred by LRIG1 expression was only observed for LMO7-negative cases.

LRIG1 significantly reduced the clonogenicity of NSCLC cell lines, which may translate into reduced metastatic potential *in vivo*. No consistent effects of LRIG1 overexpression were observed on cell migration *in vitro* and the proliferation rates of most cell lines were also unaffected. Because most of the available NSCLC cell lines are established from advanced disease, it may be necessary to develop other model systems in order to study mechanisms in early-stage disease.

Acknowledgements

When a PhD project has been going on for as many years as mine has done, in parallel with a transition from medical school all the way to being an oncology resident, it is impossible to sum up the enormous crowd of people that I have worked with along the way. For all the coworkers, research collaborators and breakroom friends not listed here, please be assured that I have appreciated you as well.

First, my thanks go to Mikael Johansson. I have been immensely fortunate to have a main supervisor who is not only a multi-skilled translational researcher and a clinical role model, but also a great friend and a kickass cook. He has gone above and beyond in supporting me and laying out the path not only for my PhD project, but also thinking ahead and helping me juggle two careers. In the future, I hope the two of us will spend less time agonizing over experiments in the lab and more time kayaking.

Håkan Hedman has not only been an incredible co-supervisor, he is also the person who got me into oncology research to start with. I literally went from never having set foot in a cell culture lab to doing full-fledged cell biology research during my time at the lab, and Håkan has been an invaluable guiding beacon in this process. I never cease to be amazed at his superpowers in turning the most jumbled and confusing manuscript into crystal clear academic writing.

Thanks to all my coworkers at the lab; especially Terese Karlsson and Camilla Holmlund who I have worked closely with on most of my papers, as well as our lab technicians Annika Holmberg, Yvonne Jonsson and Charlotte Nordström who I have put to work quite a bit over the years, and all the other members that have been in the LRIG group over the years: Carl Herdenberg, Feng Mao, Mahmood Faraz, Alexandra Lorenzzi Löfgren, Ahmad Abdullah Nasir and Ola Billing. Also, thanks to our all-knowing, all-seeing and immensely friendly administrator, Maria Wing.

Thanks to Patrick Micke and Johan Botling at the Department of Immunology, Genetics and Pathology in Uppsala for the collaboration that provided a considerable part of the data this thesis is based on. I am also thankful for the collaborations I have had with Jonas Nilsson, Emma Persson, David Lindqvist, Daniel Öhlund and all the people in their respective groups at the Oncology Research Lab, as well as the statistical gurus that have helped me over the years: Björn Tavelin, Carl Wibom and Justin Harbs. My special thanks go to Parviz Behnam Motlagh and Pernilla Andersson at Medical Biosciences, who

have gone above and beyond in helping me every time I have struggled with new methods. And, not to forget, all the incredible people I have had a laugh with in the breakroom and at our parties over these ten years: Lee-Ann Tjon, Thais Langer, Britta Söderkvist, Anna Chiara Pirona, Erik Bovinder Ylitalo, Simona Sterbova, Joshua Cumming, Tommy Lidström, Nick Karlowtaz, Alva Hansson… the list is long and, unfortunately, incomplete.

On the clinical side of things, I would especially like to mention the people I have pestered with requests for more research time, sometimes with short notice and at the most inopportune moments. I never got a no. Laila Karlsson, Elisabeth O Karlsson and Stina Lindblad, you all have my very sincerest thanks and appreciation.

My thanks also go to the very large group of doctors and other staff at Cancercentrum NUS, for being all kinds of lovely and helpful people. I often say that a bad day at the oncology clinic is like the best day at any other clinic, and this has been a key factor in my career choices both regarding clinic work and research.

Without my friends outside the work bubble, I would probably have gone mad. Thanks to Albin & Lotta, Amar & Nina, Samuel & Henny, Anders & Saga, Adrian, Maria, Giedre, Frida, Hedvig, Johan and Marcus, just to name a few.

Finally, thanks to my family and relatives for always being there for me. Robert, you mean the world to me.

References

1. Bray F, Ferlay J, Soerjomataram I, Siegel RL, Torre LA, Jemal A. Global cancer statistics 2018: GLOBOCAN estimates of incidence and mortality worldwide for 36 cancers in 185 countries. CA Cancer J Clin. 2018 Sep 12;68(6):394–424.

2. Engholm G, Ferlay J, Christensen N, Bray F, Gjerstorff ML, Klint Å, et al. NORDCAN – a Nordic tool for cancer information, planning, quality control and research. Acta Oncol. 2010 Jun;49(5):725–36.

3. Samet JM, Avila-Tang E, Boffetta P, Hannan LM, Olivo-Marston S, Thun MJ, et al. Lung cancer in never smokers: clinical epidemiology and environmental risk factors. Clin Cancer Res. American Association for Cancer Research; 2009 Sep 15;15(18):5626–45.

4. Brennan P, Crispo A, Zaridze D, Szeszenia-Dabrowska N, Rudnai P, Lissowska J, et al. High Cumulative Risk of Lung Cancer Death among Smokers and Nonsmokers in Central and Eastern Europe. Am J Epidemiol. 2006 Oct 13;164(12):1233–41.

5. Alberg AJ, Ford JG, Samet JM, American College of Chest Physicians. Epidemiology of lung cancer: ACCP evidence-based clinical practice guidelines (2nd edition). Chest. 2007 Sep;132(3 Suppl):29S–55S.

6. Walters S, Maringe C, Coleman MP, Peake MD, Butler J, Young N, et al. Lung cancer survival and stage at diagnosis in Australia, Canada, Denmark, Norway, Sweden and the UK: a population-based study, 2004-2007. Thorax. 2013 Jun;68(6):551–64.

7. Nationella lungcancerregistret. Lungcancer – Nationell kvalitetsrapport för 2019 [Internet]. 2019 ed. Wagenius G, editor. Nationellt kvalitetsregister för lungcancer. 2020 [cited 2020 Oct 14]. Available from: https://www.cancercentrum.se/globalassets/cancerdiagnoser/lunga-och-lungsack/kvalitetsregister/rapport/20200910_nlcr_nationell_rapport_2019.pdf

8. Travis WD, Brambilla E, Noguchi M, Nicholson AG, Geisinger KR, Yatabe Y, et al. International association for the study of lung cancer/american thoracic society/european respiratory society international multidisciplinary classification of lung adenocarcinoma. J Thorac Oncol. 2011 Feb;6(2):244–85.

9. Thun MJ, Lally CA, Flannery JT, Calle EE, Flanders WD, Heath CW. Cigarette smoking and changes in the histopathology of lung cancer. J Natl Cancer Inst. 1997 Nov 5;89(21):1580–6.

10. Cheng T-YD, Cramb SM, Baade PD, Youlden DR, Nwogu C, Reid ME. The International Epidemiology of Lung Cancer: Latest Trends, Disparities, and Tumor Characteristics. J Thorac Oncol. 2016 Oct;11(10):1653–71.

11. Detterbeck FC, Boffa DJ, Kim AW, Tanoue LT. The Eighth Edition Lung Cancer Stage Classification. Chest. 2017 Jan;151(1):193–203.

12. Pignon J-P, Tribodet H, Scagliotti GV, Douillard J-Y, Shepherd FA, Stephens RJ, et al. Lung adjuvant cisplatin evaluation: a pooled analysis by the LACE Collaborative Group. J Clin Oncol. 2008 Jul 20;26(21):3552–9.

13. Burdett S, Pignon J-P, Tierney J, Tribodet H, Stewart L, Le Péchoux C, et al. Adjuvant chemotherapy for resected early-stage non-small cell lung cancer. Cochrane Database Syst Rev. 2015 Mar 2;(3):CD011430.

14. Onishi H, Shirato H, Nagata Y, Hiraoka M, Fujino M, Gomi K, et al. Stereotactic body radiotherapy (SBRT) for operable stage I non-small-cell lung cancer: can SBRT be comparable to surgery? Int J Radiat Oncol Biol Phys. 2011 Dec 1;81(5):1352–8.

15. Aupérin A, Le Péchoux C, Rolland E, Curran WJ, Furuse K, Fournel P, et al. Meta-analysis of concomitant versus sequential radiochemotherapy in locally advanced non-small-cell lung cancer. J Clin Oncol. 2010 May 1;28(13):2181–90.

16. O'Rourke N, Roqué i Figuls M, Farré Bernadó N, Macbeth F. Concurrent chemoradiotherapy in non-small cell lung cancer. Cochrane Lung Cancer Group, editor. Cochrane Database Syst Rev. John Wiley & Sons, Ltd; 2010 Jun 16;35(4):195–103.

17. Yoon SM, Shaikh T, Hallman M. Therapeutic management options for stage III non-small cell lung cancer. World J Clin Oncol. 2017 Feb 10;8(1):1–20.

18. Antonia SJ, Villegas A, Daniel D, Vicente D, Murakami S, Hui R, et al. Overall Survival with Durvalumab after Chemoradiotherapy in Stage III NSCLC. N Engl J Med. 2018 Dec 13;379(24):2342–50.

19. Paz-Ares L, Spira A, Raben D, Planchard D, Cho BC, Özgüroğlu M, et al. Outcomes with durvalumab by tumour PD-L1 expression in unresectable, stage III non-small-cell lung cancer in the PACIFIC trial. Ann Oncol. 2020 Mar 21;31(6):798–806.

20. Manser R, Wright G, Hart D, Byrnes G, Campbell DA. Surgery for early stage non-small cell lung cancer. Cochrane Database Syst Rev. 2005 Jan 25;(1):CD004699.

21. Fairchild A, Harris K, Barnes E, Wong R, Lutz S, Bezjak A, et al. Palliative thoracic radiotherapy for lung cancer: a systematic review. J Clin Oncol. 2008 Aug 20;26(24):4001–11.

22. Dasari S, Tchounwou PB. Cisplatin in cancer therapy: molecular mechanisms of action. Eur J Pharmacol. 2014 Oct 5;740:364–78.

23. Roskoski R. Properties of FDA-approved small molecule protein kinase inhibitors. Pharmacol Res. 2019 Jun;144:19–50.

24. Park K, Tan EH, O'Byrne K, Zhang L, Boyer M, Mok T, et al. Afatinib versus gefitinib as first-line treatment of patients with EGFR mutation-positive non-small-cell lung cancer (LUX-Lung 7): a phase 2B, open-label, randomised controlled trial. Lancet Oncol. 2016 May;17(5):577–89.

25. Wu Y-L, Cheng Y, Zhou X, Lee KH, Nakagawa K, Niho S, et al. Dacomitinib versus gefitinib as first-line treatment for patients with EGFR-mutation-positive non-small-cell lung cancer (ARCHER 1050): a randomised, open-label, phase 3 trial. Lancet Oncol. 2017 Nov;18(11):1454–66.

26. Soria J-C, Tan DSW, Chiari R, Wu Y-L, Paz-Ares L, Wolf J, et al. First-line ceritinib versus platinum-based chemotherapy in advanced ALK-rearranged non-small-cell lung cancer (ASCEND-4): a randomised, open-label, phase 3 study. Lancet. 2017 Mar 4;389(10072):917–29.

27. Peters S, Camidge DR, Shaw AT, Gadgeel S, Ahn JS, Kim D-W, et al. Alectinib versus Crizotinib in Untreated ALK-Positive Non-Small-Cell Lung Cancer. N Engl J Med. 2017 Aug 31;377(9):829–38.

28. Camidge DR, Kim HR, Ahn M-J, Yang JC-H, Han J-Y, Lee JS, et al. Brigatinib versus Crizotinib in ALK-Positive Non-Small-Cell Lung Cancer. N Engl J Med. 2018 Nov 22;379(21):2027–39.

29. Al-Moundhri M, O'Brien M, Souberbielle BE. Immunotherapy in lung cancer. Br J Cancer. 1998 Aug;78(3):282–8.

30. Hodi FS, O'Day SJ, McDermott DF, Weber RW, Sosman JA, Haanen JB, et al. Improved survival with ipilimumab in patients with metastatic melanoma. N Engl J Med. 2010 Aug 19;363(8):711–23.

31. Walker LSK, Sansom DM. The emerging role of CTLA4 as a cell-extrinsic regulator of T cell responses. Nat Rev Immunol. 2011 Nov 25;11(12):852–63.

32. Ritprajak P, Azuma M. Intrinsic and extrinsic control of expression of the immunoregulatory molecule PD-L1 in epithelial cells and squamous cell carcinoma. Oral Oncol. 2015 Mar 1;51(3):221–8.

33. Weber J. Ipilimumab: controversies in its development, utility and autoimmune adverse events. Cancer Immunol Immunother. 2009 May;58(5):823–30.

34. O'Day SJ, Maio M, Chiarion-Sileni V, Gajewski TF, Pehamberger H, Bondarenko IN, et al. Efficacy and safety of ipilimumab monotherapy in patients with pretreated advanced melanoma: a multicenter single-arm phase II study. Ann Oncol. 2010 Aug;21(8):1712–7.

35. Hellmann MD, Paz-Ares L, Bernabe Caro R, Zurawski B, Kim S-W, Carcereny Costa E, et al. Nivolumab plus Ipilimumab in Advanced Non-Small-Cell Lung Cancer. N Engl J Med. 2019 Nov 21;381(21):2020–31.

36. Hellmann MD, Ciuleanu T-E, Pluzanski A, Lee JS, Otterson GA, Audigier-Valette C, et al. Nivolumab plus Ipilimumab in Lung Cancer with a High Tumor Mutational Burden. N Engl J Med. 2018 May 31;378(22):2093–104.

37. Wherry EJ. T cell exhaustion. Nat Immunol. 2011 Jun;12(6):492–9.

38. Ishida Y, Agata Y, Shibahara K, Honjo T. Induced expression of PD-1, a novel member of the immunoglobulin gene superfamily, upon programmed cell death. EMBO J. 1992 Nov;11(11):3887–95.

39. Karwacz K, Bricogne C, MacDonald D, Arce F, Bennett CL, Collins M, et al. PD-L1 co-stimulation contributes to ligand-induced T cell receptor down-modulation on CD8+ T cells. EMBO Mol Med. 2011 Oct;3(10):581–92.

40. Naidoo J, Page DB, Li BT, Connell LC, Schindler K, Lacouture ME, et al. Toxicities of the anti-PD-1 and anti-PD-L1 immune checkpoint antibodies. Ann Oncol. 2015 Dec;26(12):2375–91.

41. Paz-Ares L, Luft A, Vicente D, Tafreshi A, Gümüş M, Mazieres J, et al. Pembrolizumab plus Chemotherapy for Squamous Non-Small-Cell Lung Cancer. N Engl J Med. 2018 Nov 22;379(21):2040–51.

42. Gandhi L, Rodríguez-Abreu D, Gadgeel S, Esteban E, Felip E, De Angelis F, et al. Pembrolizumab plus Chemotherapy in Metastatic Non-Small-Cell Lung Cancer. N Engl J Med. 2018 May 31;378(22):2078–92.

43. West H, McCleod M, Hussein M, Morabito A, Rittmeyer A, Conter HJ, et al. Atezolizumab in combination with carboplatin plus nab-paclitaxel chemotherapy compared with chemotherapy alone as first-line treatment for metastatic non-squamous non-small-cell lung cancer (IMpower130): a multicentre, randomised, open-label, phase 3 trial. Lancet Oncol. 2019 Jul;20(7):924–37.

44. Reck M, Rodríguez-Abreu D, Robinson AG, Hui R, Csőszi T, Fülöp A, et al. Pembrolizumab versus Chemotherapy for PD-L1-Positive Non-Small-Cell Lung Cancer. N Engl J Med. 2016 Nov 10;375(19):1823–33.

45. Chansky K, Sculier J-P, Crowley JJ, Giroux D, Van Meerbeeck J, Goldstraw P, et al. The International Association for the Study of Lung Cancer Staging Project: prognostic factors and pathologic TNM stage in surgically managed non-small cell lung cancer. J Thorac Oncol. 2009 Jul;4(7):792–801.

46. Oken MM, Creech RH, Tormey DC, Horton J, Davis TE, McFadden ET, et al. Toxicity and response criteria of the Eastern Cooperative Oncology Group. Am J Clin Oncol. 1982 Dec;5(6):649–55.

47. Zheng Z, Chen T, Li X, Haura E, Sharma A, Bepler G. DNA synthesis and repair genes RRM1 and ERCC1 in lung cancer. N Engl J Med. 2007 Feb 22;356(8):800–8.

48. Rosell R, Skrzypski M, Jassem E, Taron M, Bartolucci R, Sanchez JJ, et al. BRCA1: a novel prognostic factor in resected non-small-cell lung cancer. PLoS ONE. 2007 Nov 7;2(11):e1129.

49. Reiman T, Lai R, Veillard AS, Paris E, Soria JC, Rosell R, et al. Cross-validation study of class III beta-tubulin as a predictive marker for benefit from adjuvant chemotherapy in resected non-small-cell lung cancer: analysis of four randomized trials. Ann Oncol. 2012 Jan;23(1):86–93.

50. Thakur MK, Gadgeel SM. Predictive and Prognostic Biomarkers in Non-Small Cell Lung Cancer. Semin Respir Crit Care Med. 2016 Oct;37(5):760–70.

51. Chen H-Y, Yu S-L, Chen C-H, Chang G-C, Chen C-Y, Yuan A, et al. A Five-Gene Signature and Clinical Outcome in Non–Small-Cell Lung Cancer. N Engl J Med. 2007 Jan 4;356(1):11–20.

52. Kratz JR, Haro GJ, Cook NR, He J, Van Den Eeden SK, Woodard GA, et al. Incorporation of a Molecular Prognostic Classifier Improves Conventional Non–Small Cell Lung Cancer Staging. J Thor Oncol. 2019 Jul;14(7):1223–32.

53. Zhu CQ, Ding K, Strumpf D, Weir BA, Meyerson M, Pennell N, et al. Prognostic and Predictive Gene Signature for Adjuvant Chemotherapy in Resected Non–Small-Cell Lung Cancer. JCO. 2010 Oct 10;28(29):4417–24.

54. Grieve S, Ding K, Moore J, Finniss M, Ray A, Lees M, et al. Immunohistochemical validation study of 15-gene biomarker panel predictive of benefit from adjuvant chemotherapy in resected non-small-cell lung cancer: analysis of JBR.10. ESMO Open. 2020 Mar;5(2):e000679.

55. Hirsch FR, Scagliotti GV, Mulshine JL, Kwon R, Curran WJ, Wu Y-L, et al. Lung cancer: current therapies and new targeted treatments. Lancet. 2017 Jan 21;389(10066):299–311.

56. Vatansever S, Erman B, Gümüş ZH. Oncogenic G12D mutation alters local conformations and dynamics of K-Ras. Sci Rep. 2019 Aug 13;9(1):11730.

57. Brugger W, Triller N, Blasinska-Morawiec M, Curescu S, Sakalauskas R, Manikhas GM, et al. Prospective molecular marker analyses of EGFR and KRAS from a randomized, placebo-controlled study of erlotinib maintenance therapy in advanced non-small-cell lung cancer. J Clin Oncol. 2011 Nov 1;29(31):4113–20.

58. Johnson ML, Sima CS, Chaft J, Paik PK, Pao W, Kris MG, et al. Association of KRAS and EGFR mutations with survival in patients with advanced lung adenocarcinomas. Cancer. 2013 Jan 15;119(2):356–62.

59. AMG 510 First to Inhibit "Undruggable" KRAS. Cancer Discov. 2019 Aug;9(8):988–9.

60. Altaha R, Liang X, Yu JJ, Reed E. Excision repair cross complementing-group 1: gene expression and platinum resistance. Int J Mol Med. 2004 Dec;14(6):959–70.

61. Lord RVN, Brabender J, Gandara D, Alberola V, Camps C, Domine M, et al. Low ERCC1 expression correlates with prolonged survival after cisplatin plus gemcitabine chemotherapy in non-small cell lung cancer. Clin Cancer Res. 2002 Jul;8(7):2286–91.

62. Choi CM, Yang SC, Jo HJ, Song SY, Jeon YJ, Jang TW, et al. Proteins involved in DNA damage response pathways and survival of stage I non-small-cell lung cancer patients. Ann Oncol. 2012 Aug;23(8):2088–93.

63. Bergman AM, Eijk PP, Ruiz van Haperen VWT, Smid K, Veerman G, Hubeek I, et al. In vivo Induction of Resistance to Gemcitabine Results in Increased Expression of Ribonucleotide Reductase Subunit M1 as the Major Determinant. Cancer Res. 2005 Oct 17;65(20):9510–6.

64. Rosell R, Danenberg KD, Alberola V, Bepler G, Sanchez JJ, Camps C, et al. Ribonucleotide reductase messenger RNA expression and survival in gemcitabine/cisplatin-treated advanced non-small cell lung cancer patients. Clin Cancer Res. 2004 Feb;10(4):1318–25.

65. Bepler G, Olaussen KA, Vataire A-L, Soria J-C, Zheng Z, Dunant A, et al. ERCC1 and RRM1 in the International Adjuvant Lung Trial by Automated Quantitative in Situ Analysis. Am J Pathol. 2011 Jan;178(1):69–78.

66. Friboulet L, Olaussen KA, Pignon J-P, Shepherd FA, Tsao M-S, Graziano S, et al. ERCC1 isoform expression and DNA repair in non-small-cell lung cancer. N Engl J Med. 2013 Mar;368(12):1101–10.

67. Wachters FM, Wong LSM, Timens W, Kampinga HH, Groen HJM. ERCC1, hRad51, and BRCA1 protein expression in relation to tumour response and survival of stage III/IV NSCLC patients treated with chemotherapy. Lung Cancer. 2005 Nov;50(2):211–9.

68. Wang L, Wei J, Qian X, Yin H, Zhao Y, Yu L, et al. ERCC1 and BRCA1 mRNA expression levels in metastatic malignant effusions is associated with chemosensitivity to cisplatin and/or docetaxel. BMC Cancer. 2008 Apr 11;8:97.

69. Yang Y, Xie Y, Xian L. Breast cancer susceptibility gene 1 (BRCA1) predict clinical outcome in platinum- and toxal-based chemotherapy in non-small-cell lung cancer (NSCLC) patients: a system review and meta-analysis. J Exp Clin Cancer Res. 2013 Mar 15;32(1):15–9.

70. Wei J, Cobo M, Domine M, Chaib I, You C, Massuti B, et al. Two biomarker-directed randomized trials in European and Chinese patients with nonsmall-cell lung cancer: the BRCA1-RAP80 Expression Customization (BREC) studies. Ann Oncol. 2014 Nov;25(11):2147–55.

71. Sève P, Mackey J, Isaac S, Trédan O, Souquet P-J, Pérol M, et al. Class III beta-tubulin expression in tumor cells predicts response and outcome in patients with non-small cell lung cancer receiving paclitaxel. Mol Cancer Ther. 2005 Dec;4(12):2001–7.

72. Edelman MJ, Schneider C-P, Tsai C-M, Kim H-T, Quoix E, Luft AV, et al. Randomized Phase II Study of Ixabepilone or Paclitaxel Plus Carboplatin in Patients With Non–Small-Cell Lung Cancer Prospectively Stratified by Beta-3 Tubulin Status. JCO. 2013 Jun 1;31(16):1990–6.

73. Barlesi F, Mazieres J, Merlio J-P, Debieuvre D, Mosser J, Lena H, et al. Routine molecular profiling of patients with advanced non-small-cell lung cancer: results of a 1-year nationwide programme of the French Cooperative Thoracic Intergroup (IFCT). Lancet. 2016 Apr 2;387(10026):1415–26.

74. Lovly C, L Horn V, Pao W. Molecular Profiling of Lung Cancer. [Internet]. My Cancer Genome. 2018 [cited 2018 Oct 23]. Available from: https://www.mycancergenome.org/content/disease/lung-cancer/

75. Köhn L, Johansson M, Grankvist K, Nilsson J. Liquid biopsies in lung cancer—time to implement research technologies in routine care? Ann Transl Med. 2017 Jul;5(13):278–8.

76. Chu QS. Targeting non-small cell lung cancer: driver mutation beyond epidermal growth factor mutation and anaplastic lymphoma kinase fusion. Ther Adv Med Oncol. 2020;12:1758835919895756.

77. Dutt A, Ramos AH, Hammerman PS, Mermel C, Cho J, Sharifnia T, et al. Inhibitor-sensitive FGFR1 amplification in human non-small cell lung cancer. PLoS ONE. 2011;6(6):e20351.

78. Turner NC, Seckl MJ. A therapeutic target for smoking-associated lung cancer. Sci Transl Med. 2010 Dec 15;2(62):62ps56–6.

79. Weiss J, Sos ML, Seidel D, Peifer M, Zander T, Heuckmann JM, et al. Frequent and focal FGFR1 amplification associates with therapeutically tractable FGFR1 dependency in squamous cell lung cancer. Sci Transl Med. 2010 Dec 15;2(62):62ra93–3.

80. Lovly C, L Horn V, Pao W. KRAS in Non-Small Cell Lung Cancer (NSCLC) [Internet]. My Cancer Genome. 2015 [cited 2018 Oct 23]. Available from: https://www.mycancergenome.org/content/disease/lung-cancer/kras/

81. Sharma SV, Bell DW, Settleman J, Haber DA. Epidermal growth factor receptor mutations in lung cancer. Nat Rev Cancer. 2007 Mar;7(3):169–81.

82. Gainor JF, Varghese AM, Ou S-HI, Kabraji S, Awad MM, Katayama R, et al. ALK rearrangements are mutually exclusive with mutations in EGFR or KRAS: an analysis of 1,683 patients with non-small cell lung cancer. Clin Cancer Res. 2013 Aug 1;19(15):4273–81.

83. Drilon A, Laetsch TW, Kummar S, DuBois SG, Lassen UN, Demetri GD, et al. Efficacy of Larotrectinib in TRK Fusion-Positive Cancers in Adults and Children. N Engl J Med. 2018 Feb 22;378(8):731–9.

84. Drilon A, Oxnard GR, Tan DSW, Loong HHF, Johnson M, Gainor J, et al. Efficacy of Selpercatinib in RET Fusion-Positive Non-Small-Cell Lung Cancer. N Engl J Med. 2020 Aug 27;383(9):813–24.

85. Ullrich A, Coussens L, Hayflick JS, Dull TJ, Gray A, Tam AW, et al. Human epidermal growth factor receptor cDNA sequence and aberrant expression of the amplified gene in A431 epidermoid carcinoma cells. Nature. 1984 Jun;309(5967):418–25.

86. Olayioye MA, Neve RM, Lane HA, Hynes NE. The ErbB signaling network: receptor heterodimerization in development and cancer. EMBO J. 2000 Jul 3;19(13):3159–67.

87. Qian X, LeVea CM, Freeman JK, Dougall WC, Greene MI. Heterodimerization of epidermal growth factor receptor and wild-type or kinase-deficient Neu: a mechanism of interreceptor kinase activation and transphosphorylation. Proc Natl Acad Sci USA. 1994 Feb 15;91(4):1500–4.

88. Karunagaran D, Tzahar E, Beerli RR, Chen X, Graus-Porta D, Ratzkin BJ, et al. ErbB-2 is a common auxiliary subunit of NDF and EGF receptors: implications for breast cancer. EMBO J. 1996 Jan 15;15(2):254–64.

89. Cohen S, Ushiro H, Stoscheck C, Chinkers M. A native 170,000 epidermal growth factor receptor-kinase complex from shed plasma membrane vesicles. J Biol Chem. 1982 Feb 10;257(3):1523–31.

90. Yarden Y, Schlessinger J. Epidermal growth factor induces rapid, reversible aggregation of the purified epidermal growth factor receptor. Biochemistry. 1987 Mar 10;26(5):1443–51.

91. Sherwin SA, Minna JD, Gazdar AF, Todaro GJ. Expression of epidermal and nerve growth factor receptors and soft agar growth factor production by human lung cancer cells. Cancer Res. 1981 Sep;41(9 Pt 1):3538–42.

92. Cerny T, Barnes DM, Hasleton P, Barber PV, Healy K, Gullick W, et al. Expression of epidermal growth factor receptor (EGF-R) in human lung tumours. Br J Cancer. 1986 Aug;54(2):265–9.

93. Veale D, Ashcroft T, Marsh C, Gibson GJ, Harris AL. Epidermal growth factor receptors in non-small cell lung cancer. Br J Cancer. 1987 May;55(5):513–6.

94. Lynch TJ, Bell DW, Sordella R, Gurubhagavatula S, Okimoto RA, Brannigan BW, et al. Activating mutations in the epidermal growth factor receptor underlying responsiveness of non-small-cell lung cancer to gefitinib. N Engl J Med. 2004 May 20;350(21):2129–39.

95. Paez JG, Jänne PA, Lee JC, Tracy S, Greulich H, Gabriel S, et al. EGFR Mutations in Lung Cancer: Correlation with Clinical Response to Gefitinib Therapy. Science. 2004 Jun 4;304(5676):1497–500.

96. Pao W, Miller V, Zakowski M, Doherty J, Politi K, Sarkaria I, et al. EGF receptor gene mutations are common in lung cancers from "never smokers" and are associated with sensitivity of tumors to gefitinib and erlotinib. Proc Natl Acad Sci USA. 2004 Sep 7;101(36):13306–11.

97. Kumar A, Petri ET, Halmos B, Boggon TJ. Structure and clinical relevance of the epidermal growth factor receptor in human cancer. J Clin Oncol. 2008 Apr 1;26(10):1742–51.

98. Yarden Y, Sliwkowski MX. Untangling the ErbB signalling network. Nat Rev Mol Cell Biol. 2001 Feb;2(2):127–37.

99. Mok TS, Wu Y-L, Ahn M-J, Garassino MC, Kim HR, Ramalingam SS, et al. Osimertinib or Platinum–Pemetrexed in EGFRT790M–Positive Lung Cancer. N Engl J Med. 2017 Feb 16;376(7):629–40.

100. Chiba M, Togashi Y, Bannno E, Kobayashi Y, Nakamura Y, Hayashi H, et al. Efficacy of irreversible EGFR-TKIs for the uncommon secondary resistant EGFR mutations L747S, D761Y, and T854A. BMC Cancer. 2017 Apr 19;17(1):281.

101. Yu HA, Tian SK, Drilon AE, Borsu L, Riely GJ, Arcila ME, et al. Acquired Resistance of EGFR-Mutant Lung Cancer to a T790M-Specific EGFR Inhibitor: Emergence of a Third Mutation (C797S) in the EGFR Tyrosine Kinase Domain. JAMA Oncol. 2015 Oct;1(7):982–4.

102. Engelman JA, Zejnullahu K, Mitsudomi T, Song Y, Hyland C, Park JO, et al. MET Amplification Leads to Gefitinib Resistance in Lung Cancer by Activating ERBB3 Signaling. Science. 2007 May 18;316(5827):1039–43.

103. Sequist LV, Waltman BA, Dias-Santagata D, Digumarthy S, Turke AB, Fidias P, et al. Genotypic and histological evolution of lung cancers acquiring resistance to EGFR inhibitors. Sci Transl Med. 2011 Mar 23;3(75):75ra26–6.

104. Yano S, Wang W, Li Q, Matsumoto K, Sakurama H, Nakamura T, et al. Hepatocyte growth factor induces gefitinib resistance of lung adenocarcinoma with epidermal growth factor receptor-activating mutations. Cancer Res. 2008 Nov 15;68(22):9479–87.

105. Takezawa K, Pirazzoli V, Arcila ME, Nebhan CA, Song X, de Stanchina E, et al. HER2 amplification: a potential mechanism of acquired resistance to EGFR inhibition in EGFR-mutant lung cancers that lack the second-site EGFRT790M mutation. Cancer Discov. 2012 Oct;2(10):922–33.

106. Zhang Z, Lee JC, Lin L, Olivas V, Au V, LaFramboise T, et al. Activation of the AXL kinase causes resistance to EGFR-targeted therapy in lung cancer. Nat Genet. 2012 Jul 1;44(8):852–60.

107. Oser MG, Niederst MJ, Sequist LV, Engelman JA. Transformation from non-small-cell lung cancer to small-cell lung cancer: molecular drivers and cells of origin. Lancet Oncol. 2015 Apr;16(4):e165–72.

108. Marcoux N, Gettinger SN, O'Kane G, Arbour KC, Neal JW, Husain H, et al. EGFR-Mutant Adenocarcinomas That Transform to Small-Cell Lung Cancer and Other Neuroendocrine Carcinomas: Clinical Outcomes. J Clin Oncol. 2018 Dec 14;37(4):JCO1801585–285.

109. Reshetnyak AV, Murray PB, Shi X, Mo ES, Mohanty J, Tome F, et al. Augmentor α and β (FAM150) are ligands of the receptor tyrosine kinases ALK and LTK: Hierarchy and specificity of ligand–receptor interactions. Proc Natl Acad Sci USA. 2015 Dec 29;112(52):15862–7.

110. Fadeev A, Mendoza-Garcia P, Irion U, Guan J, Pfeifer K, Wiessner S, et al. ALKALs are in vivo ligands for ALK family receptor tyrosine kinases in the neural crest and derived cells. Proc Natl Acad Sci USA. 2018 Jan 23;115(4):E630–8.

111. Wolfstetter G, Pfeifer K, van Dijk JR, Hugosson F, Lu X, Palmer RH. The scaffolding protein Cnk binds to the receptor tyrosine kinase Alk to promote visceral founder cell specification in Drosophila. Sci Signal. 2017 Oct 24;10(502):eaan0804.

112. Palmer RH, Vernersson E, Grabbe C, Hallberg B. Anaplastic lymphoma kinase: signalling in development and disease. Biochem J. 2009 May 27;420(3):345–61.

113. Hallberg B, Palmer RH. Mechanistic insight into ALK receptor tyrosine kinase in human cancer biology. Nat Rev Cancer. 2013 Oct;13(10):685–700.

114. Soda M, Choi YL, Enomoto M, Takada S, Yamashita Y, Ishikawa S, et al. Identification of the transforming EML4-ALK fusion gene in non-small-cell lung cancer. Nature. 2007 Aug 2;448(7153):561–6.

115. Takeuchi K, Choi YL, Soda M, Inamura K, Togashi Y, Hatano S, et al. Multiplex reverse transcription-PCR screening for EML4-ALK fusion transcripts. Clin Cancer Res. 2008 Oct 15;14(20):6618–24.

116. Sasaki T, Rodig SJ, Chirieac LR, Jänne PA. The biology and treatment of EML4-ALK non-small cell lung cancer. Eur J Cancer. 2010 Jul;46(10):1773–80.

117. Mano H. ALKoma: a cancer subtype with a shared target. Cancer Discov. 2012 Jun;2(6):495–502.

118. Shaw AT, Solomon B. Targeting Anaplastic Lymphoma Kinase in Lung Cancer. Clin Cancer Res. 2011 Apr 14;17(8):2081–6.

119. Rikova K, Guo A, Zeng Q, Possemato A, Yu J, Haack H, et al. Global Survey of Phosphotyrosine Signaling Identifies Oncogenic Kinases in Lung Cancer. Cell. 2007 Dec;131(6):1190–203.

120. Bergethon K, Shaw AT, Ou S-HI, Katayama R, Lovly CM, McDonald NT, et al. ROS1 rearrangements define a unique molecular class of lung cancers. J Clin Oncol. 2012 Mar 10;30(8):863–70.

121. Davies KD, Le AT, Theodoro MF, Skokan MC, Aisner DL, Berge EM, et al. Identifying and targeting ROS1 gene fusions in non-small cell lung cancer. Clin Cancer Res. 2012 Sep 1;18(17):4570–9.

122. Soda M, Togashi Y, Suzuki R, Sakata S, Hatano S, Asaka R, et al. RET, ROS1 and ALK fusions in lung cancer. Nat Med. 2012 Feb 12;18(3):378–81.

123. Doebele RC, Pilling AB, Aisner DL, Kutateladze TG, Le AT, Weickhardt AJ, et al. Mechanisms of resistance to crizotinib in patients with ALK gene rearranged non-small cell lung cancer. Clin Cancer Res. 2012 Mar;18(5):1472–82.

124. Katayama R, Shaw AT, Khan TM, Mino-Kenudson M, Solomon BJ, Halmos B, et al. Mechanisms of acquired crizotinib resistance in ALK-rearranged lung Cancers. Sci Transl Med. 2012 Feb 8;4(120):120ra17–7.

125. McCoach CE, Le AT, Gowan K, Jones K, Schubert L, Doak A, et al. Resistance Mechanisms to Targeted Therapies in ROS1+ and ALK+ Non-small Cell Lung Cancer. Clin Cancer Res. 2018 Jul 15;24(14):3334–47.

126. Lin JJ, Shaw AT. Recent Advances in Targeting ROS1 in Lung Cancer. J Thorac Oncol. 2017 Nov;12(11):1611–25.

127. Organ SL, Tsao M-S. An overview of the c-MET signaling pathway. Ther Adv Med Oncol. 2011 Nov;3(1 Suppl):S7–S19.

128. Awad MM. Impaired c-Met Receptor Degradation Mediated by MET Exon 14 Mutations in Non-Small-Cell Lung Cancer. J Clin Oncol. 2016 Mar 10;34(8):879–81.

129. Drilon A, Clark JW, Weiss J, Ou S-HI, Camidge DR, Solomon BJ, et al. Antitumor activity of crizotinib in lung cancers harboring a MET exon 14 alteration. Nat Med. 2020 Jan;26(1):47–51.

130. Davies H, Bignell GR, Cox C, Stephens P, Edkins S, Clegg S, et al. Mutations of the BRAF gene in human cancer. Nature. 2002 Jun 27;417(6892):949–54.

131. Paik PK, Arcila ME, Fara M, Sima CS, Miller VA, Kris MG, et al. Clinical characteristics of patients with lung adenocarcinomas harboring BRAF mutations. J Clin Oncol. 2011 May 20;29(15):2046–51.

132. Alexandrov LB, Nik-Zainal S, Wedge DC, Aparicio SAJR, Behjati S, Biankin AV, et al. Signatures of mutational processes in human cancer. Nature. 2013 Aug 22;500(7463):415–21.

133. Rizvi NA, Hellmann MD, Snyder A, Kvistborg P, Makarov V, Havel JJ, et al. Cancer immunology. Mutational landscape determines sensitivity to PD-1 blockade in non-small cell lung cancer. Science. 2015 Apr 3;348(6230):124–8.

134. Goodman AM, Kato S, Bazhenova L, Patel SP, Frampton GM, Miller V, et al. Tumor Mutational Burden as an Independent Predictor of Response to Immunotherapy in Diverse Cancers. Mol Cancer Ther. 2017 Nov;16(11):2598–608.

135. Garassino M, Rodriguez-Abreu D, Gadgeel S, Esteban E, Felip E, Speranza G, et al. OA04.06 Evaluation of TMB in KEYNOTE-189: Pembrolizumab Plus Chemotherapy vs Placebo Plus Chemotherapy for Nonsquamous NSCLC. J Thor Oncol. 2019 Oct;14(10):S216–7.

136. Gainor JF, Shaw AT, Sequist LV, Fu X, Azzoli CG, Piotrowska Z, et al. EGFR Mutations and ALK Rearrangements Are Associated with Low Response Rates to PD-1 Pathway Blockade in Non-Small Cell Lung Cancer: A Retrospective Analysis. Clin Cancer Res. 2016 Sep 15;22(18):4585–93.

137. Lee CK, Man J, Lord S, Links M, Gebski V, Mok T, et al. Checkpoint Inhibitors in Metastatic EGFR-Mutated Non-Small Cell Lung Cancer-A Meta-Analysis. J Thorac Oncol. 2017 Feb;12(2):403–7.

138. Govindan R, Ding L, Griffith M, Subramanian J, Dees ND, Kanchi KL, et al. Genomic landscape of non-small cell lung cancer in smokers and never-smokers. Cell. 2012 Sep 14;150(6):1121–34.

139. Guo D, Holmlund C, Henriksson R, Hedman H. The LRIG gene family has three vertebrate paralogs widely expressed in human and mouse tissues and a homolog in Ascidiacea. Genomics. 2004 Jul;84(1):157–65.

140. Chen Y, Aulia S, Li L, Tang BL. AMIGO and friends: an emerging family of brain-enriched, neuronal growth modulating, type I transmembrane proteins with leucine-rich repeats (LRR) and cell adhesion molecule motifs. Brain Res Rev. 2006 Aug;51(2):265–74.

141. Gumienny TL, Macneil L, Zimmerman CM, Wang H, Chin L, Wrana JL, et al. Caenorhabditis elegans SMA-10/LRIG is a conserved transmembrane protein that enhances bone morphogenetic protein signaling. PLoS Genet. 2010 May 20;6(5):e1000963.

142. Gur G, Rubin C, Katz M, Amit I, Citri A, Nilsson J, et al. LRIG1 restricts growth factor signaling by enhancing receptor ubiquitylation and degradation. EMBO J. 2004 Jul 29;23(16):3270–81.

143. Laederich MB. The Leucine-rich Repeat Protein LRIG1 Is a Negative Regulator of ErbB Family Receptor Tyrosine Kinases. J Biol Chem. 2004 Aug 16;279(45):47050–6.

144. Shattuck DL, Miller JK, Laederich M, Funes M, Petersen H, Carraway KL, et al. LRIG1 Is a Novel Negative Regulator of the Met Receptor and Opposes Met and Her2 Synergy. Mol Cell Biol. 2007 Feb 13;27(5):1934–46.

145. Ledda F, Bieraugel O, Fard SS, Vilar M, Paratcha G. Lrig1 Is an Endogenous Inhibitor of Ret Receptor Tyrosine Kinase Activation, Downstream Signaling, and Biological Responses to GDNF. J Neurosci. 2008 Jan 2;28(1):39–49.

146. Faraz M, Herdenberg C, Holmlund C, Henriksson R, Hedman H. A protein interaction network centered on leucine-rich repeats and immunoglobulin-like domains 1 (LRIG1) regulates growth factor receptors. J Biol Chem. 2018 Mar 2;293(9):3421–35.

147. Alsina FC, Hita FJ, Fontanet PA, Irala D, Hedman H, Ledda F, et al. Lrig1 is a cell-intrinsic modulator of hippocampal dendrite complexity and BDNF signaling. EMBO Rep. 2016 Apr;17(4):601–16.

148. Stutz MA, Shattuck DL, Laederich MB, Carraway KL, Sweeney C. LRIG1 negatively regulates the oncogenic EGF receptor mutant EGFRvIII. Oncogene. 2008 Jun 9;27(43):5741–52.

149. Goldoni S, Iozzo RA, Kay P, Campbell S, McQuillan A, Agnew C, et al. A soluble ectodomain of LRIG1 inhibits cancer cell growth by attenuating basal and ligand-dependent EGFR activity. Oncogene. 2006 Jul 17;26(3):368–81.

150. Johansson M, Oudin A, Tiemann K, Bernard A, Golebiewska A, Keunen O, et al. The soluble form of the tumor suppressor Lrig1 potently inhibits in vivo glioma growth irrespective of EGF receptor status. Neuro Oncol. 2013 Sep;15(9):1200–11.

151. Rouam S, Moreau T, Broët P. Identifying common prognostic factors in genomic cancer studies: a novel index for censored outcomes. BMC Bioinformatics. 2010 Mar 24;11(1):150.

152. Krig SR, Frietze S, Simion C, Miller JK, Fry WHD, Rafidi H, et al. Lrig1 is an estrogen-regulated growth suppressor and correlates with longer relapse-free survival in ERα-positive breast cancer. Mol Cancer Res. 2011 Oct 16;9(10):1406–17.

153. Ljuslinder I, Malmer B, Golovleva I, Thomasson M, Grankvist K, Höckenström T, et al. Increased copy number at 3p14 in breast cancer. Breast Cancer Res. 2005;7(5):R719–27.

154. Wang Y, Poulin EJ, Coffey RJ. LRIG1 is a triple threat: ERBB negative regulator, intestinal stem cell marker and tumour suppressor. Br J Cancer. 2013 Apr 4.

155. Lindström AK, Ekman K, Stendahl U, Tot T, Henriksson R, Hedman H, et al. LRIG1 and squamous epithelial uterine cervical cancer: correlation to prognosis, other tumor markers, sex steroid hormones, and smoking. Int J Gynecol Cancer. 2008 Mar;18(2):312–7.

156. Muller SS, Lindquist DD, Kanter LL, Flores-Staino CC, Henriksson RR, Hedman HH, et al. Expression of LRIG1 and LRIG3 correlates with human papillomavirus status and patient survival in cervical adenocarcinoma. Int J Oncol. 2012 Dec 31;42(1):247–52.

157. Tanemura A, Nagasawa T, Inui S, Itami S. LRIG-1 provides a novel prognostic predictor in squamous cell carcinoma of the skin: immunohistochemical analysis for 38 cases. Dermatol Surg. 2005 Apr;31(4):423–30.

158. Sheu JJ-C, Lee C-C, Hua C-H, Li C-I, Lai M-T, Lee S-C, et al. LRIG1 modulates aggressiveness of head and neck cancers by regulating EGFR-MAPK-SPHK1 signaling and extracellular matrix remodeling. Oncogene. 2014 Mar 13;33(11):1375–84.

159. Lindquist D, Näsman A, Tarján M, Henriksson R, Tot T, Dalianis T, et al. Expression of LRIG1 is associated with good prognosis and human papillomavirus status in oropharyngeal cancer. Br J Cancer. 2014 Apr 1;110(7):1793–800.

160. Yang B, Dai C, Tan R, Zhang B, Meng X, Ye J, et al. Lrig1 is a positive prognostic marker in hepatocellular carcinoma. Onco Targets Ther. 2016;9:7071–9.

161. Wong VWY, Stange DE, Page ME, Buczacki S, Wabik A, Itami S, et al. Lrig1 controls intestinal stem-cell homeostasis by negative regulation of ErbB signalling. Nat Cell Biol. 2012 Mar 4;14(4):401–8.

162. Powell AE, Wang Y, Li Y, Poulin EJ, Means AL, Washington MK, et al. The pan-ErbB negative regulator Lrig1 is an intestinal stem cell marker that functions as a tumor suppressor. Cell. 2012 Mar 30;149(1):146–58.

163. Suzuki Y, Miura H, Tanemura A, Kobayashi K, Kondoh G, Sano S, et al. Targeted disruption of LIG-1 gene results in psoriasiform epidermal hyperplasia. FEBS Lett. 2002 Jun 19;521(1-3):67–71.

164. Xiao Q, Dong M, Cheng F, Mao F, Zong W, Wu K, et al. LRIG2 promotes the proliferation and cell cycle progression of glioblastoma cells in vitro and in vivo through enhancing PDGFRβ signaling. Int J Oncol. 2018 Sep;53(3):1069–82.

165. Xiao Q, Tan Y, Guo Y, Yang H, Mao F, Xie R, et al. Soluble LRIG2 Ectodomain Is Released from Glioblastoma Cells and Promotes the Proliferation and Inhibits the Apoptosis of Glioblastoma Cells In Vitro and In Vivo in a Similar Manner to the Full-Length LRIG2. PLoS ONE. 2014 Oct 29;9(10):e111419.

166. Abraira VE, Satoh T, Fekete DM, Goodrich LV. Vertebrate Lrig3-ErbB Interactions Occur In Vitro but Are Unlikely to Play a Role in Lrig3-Dependent Inner Ear Morphogenesis. PLoS ONE. 2010 Feb 1;5(2):e8981.

167. Rafidi H, Mercado F, Astudillo M, Fry WHD, Saldana M, Carraway KL, et al. Leucine-rich repeat and immunoglobulin domain-containing protein-1 (Lrig1) negative regulatory action toward ErbB receptor tyrosine kinases is opposed by leucine-rich repeat and immunoglobulin domain-containing protein 3 (Lrig3). J Biol Chem. 2013 Jul 26;288(30):21593–605.

168. Stuart HM, Roberts NA, Burgu B, Daly SB, Urquhart JE, Bhaskar S, et al. LRIG2 mutations cause urofacial syndrome. Am J Hum Genet. 2013 Feb 7;92(2):259–64.

169. Roberts NA, Hilton EN, Lopes FM, Singh S, Randles MJ, Gardiner NJ, et al. Lrig2 and Hpse2, mutated in urofacial syndrome, pattern nerves in the urinary bladder. Kidney Int. 2019 May;95(5):1138–52.

170. Abraira VE, Del Rio T, Tucker AF, Slonimsky J, Keirnes HL, Goodrich LV. Cross-repressive interactions between Lrig3 and netrin 1 shape the architecture of the inner ear. Development. 2008 Dec;135(24):4091–9.

171. Hedman H, Lindström AK, Tot T, Stendahl U, Henriksson R, Hellberg D. LRIG2 in contrast to LRIG1 predicts poor survival in early-stage squamous cell carcinoma of the uterine cervix. Acta Oncol. 2010 Aug;49(6):812–5.

172. Holmlund C, Haapasalo H, Yi W, Raheem O, Brännström T, Bragge H, et al. Cytoplasmic LRIG2 expression is associated with poor oligodendroglioma patient survival. Neuropathology. 2009 Jun;29(3):242–7.

173. Rondahl V, Holmlund C, Karlsson T, Wang B, Faraz M, Henriksson R, et al. Lrig2-deficient mice are protected against PDGFB-induced glioma. PLoS ONE. 2013;8(9):e73635.

174. Guo D, Nilsson J, Haapasalo H, Raheem O, Bergenheim T, Hedman H, et al. Perinuclear leucine-rich repeats and immunoglobulin-like domain proteins (LRIG1-3) as prognostic indicators in astrocytic tumors. Acta Neuropathol. 2006 Mar 11;111(3):238–46.

175. Boelens MC, van den Berg A, Fehrmann RSN, Geerlings M, de Jong WK, Meerman te GJ, et al. Current smoking-specific gene expression signature in normal bronchial epithelium is enhanced in squamous cell lung cancer. J Pathol. 2009 Jun;218(2):182–91.

176. Botling J, Edlund K, Lohr M, Hellwig B, Holmberg L, Lambe M, et al. Biomarker discovery in non-small cell lung cancer: integrating gene expression profiling, meta-analysis, and tissue microarray validation. Clin Cancer Res. 2013 Jan 1;19(1):194–204.

177. Nilsson J, Vallbo C, Guo D, Golovleva I, Hallberg B, Henriksson R, et al. Cloning, characterization, and expression of human LIG1. Biochem Biophys Res Commun. 2001 Jun 29;284(5):1155–61.

178. Holmlund C, Nilsson J, Guo D, Starefeldt A, Golovleva I, Henriksson R, et al. Characterization and tissue-specific expression of human LRIG2. Gene. 2004 May;332:35–43.

179. Uhlén M, Fagerberg L, Hallström BM, Lindskog C, Oksvold P, Mardinoglu A, et al. Proteomics. Tissue-based map of the human proteome. Science. 2015 Jan 23;347(6220):1260419–9.

180. Goldman M, Craft B, Swatloski T, Ellrott K, Cline M, Diekhans M, et al. The UCSC Cancer Genomics Browser: update 2013. Nucleic Acids Res. 2012 Dec 18;41(D1):D949–54.

181. Jamovi [Internet]. 1st ed. The Jamovi Project. Available from: https://jamovi.org

182. R: A language and environment for statistical computing [Internet]. 3rd ed. R Core Team. Available from: https://cran.r-project.org

183. Mao F, Holmlund C, Faraz M, Wang W, Bergenheim T, Kvarnbrink S, et al. Lrig1 is a haploinsufficient tumor suppressor gene in malignant glioma. Oncogenesis. 2018 Feb 2;7(2):13.

184. Gietz R, Woods R. Genetic transformation of yeast. Biotechniques. 2001 Apr;30(4):816–20.

185. Serebriiskii IG, Golemis EA. Uses of lacZ to study gene function: evaluation of beta-galactosidase assays employed in the yeast two-hybrid system. Anal Biochem. 2000 Oct 1;285(1):1–15.

186. Kolonin MG, Zhong J, Finley RL. Interaction mating methods in two-hybrid systems. Methods Enzymol. 2000;328:26–46.

187. Smith PK, Krohn RI, Hermanson GT, Mallia AK, Gartner FH, Provenzano MD, et al. Measurement of protein using bicinchoninic acid. Anal Biochem. 1985 Oct;150(1):76–85.

188. Schneider CA, Rasband WS, Eliceiri KW. NIH Image to ImageJ: 25 years of image analysis. Nat Methods. 2012 Jul;9(7):671–5.

189. Boyden S. The chemotactic effect of mixtures of antibody and antigen on polymorphonuclear leucocytes. J Exp Med. 1962 Mar 1;115(3):453–66.

190. Franken NAP, Rodermond HM, Stap J, Haveman J, van Bree C. Clonogenic assay of cells in vitro. Nat Protoc. 2006;1(5):2315–9.

191. Puck TT, Marcus PI. Action of x-rays on mammalian cells. J Exp Med. 1956 May 1;103(5):653–66.

192. Markossian S, Sittampalam GS, Grossman A, Brimacombe K, Arkin M, Auld D, et al. Cell Viability Assays. Bethesda (MD): Eli Lilly & Company and the National Center for Advancing Translational Sciences; 2004.

193. Hafner M, Niepel M, Chung M, Sorger PK. Growth rate inhibition metrics correct for confounders in measuring sensitivity to cancer drugs. Nat Methods. 2016 Jun;13(6):521–7.

194. Rhodes DR, Yu J, Shanker K, Deshpande N, Varambally R, Ghosh D, et al. ONCOMINE: a cancer microarray database and integrated data-mining platform. Neoplasia. 2004 Jan;6(1):1–6.

195. Yi W, Holmlund C, Nilsson J, Inui S, Lei T, Itami S, et al. Paracrine regulation of growth factor signaling by shed leucine-rich repeats and immunoglobulin-like domains 1. Exp Cell Res. 2011 Feb 15;317(4):504–12.

196. Feuerstein R, Wang X, Song D, Cooke NE, Liebhaber SA. The LIM/double zinc-finger motif functions as a protein dimerization domain. Proc Natl Acad Sci USA. 1994 Oct 25;91(22):10655–9.

197. Schmeichel KL, Beckerle MC. The LIM domain is a modular protein-binding interface. Cell. 1994 Oct 21;79(2):211–9.

198. Arber S, Caroni P. Specificity of single LIM motifs in targeting and LIM/LIM interactions in situ. Genes Dev. 1996 Feb 1;10(3):289–300.

199. Söderberg O, Gullberg M, Jarvius M, Ridderstråle K, Leuchowius K-J, Jarvius J, et al. Direct observation of individual endogenous protein complexes in situ by proximity ligation. Nat Methods. 2006 Dec;3(12):995–1000.

200. Ooshio T, Irie K, Morimoto K, Fukuhara A, Imai T, Takai Y. Involvement of LMO7 in the association of two cell-cell adhesion molecules, nectin and E-cadherin, through afadin and alpha-actinin in epithelial cells. J Biol Chem. 2004 Jul 23;279(30):31365–73.

201. Velthuis Te AJW, Bagowski CP. PDZ and LIM domain-encoding genes: molecular interactions and their role in development. Sci World J. 2007;7:1470–92.

202. Lehman W, Craig R, Kendrick-Jones J, Sutherland-Smith AJ. An open or closed case for the conformation of calponin homology domains on F-actin? J Muscle Res Cell Motil. 2004;25(4-5):351–8.

203. Lin Y-H, Zhen Y-Y, Chien K-Y, Lee I-C, Lin W-C, Chen M-Y, et al. LIMCH1 regulates nonmuscle myosin-II activity and suppresses cell migration. Mol Biol Cell. 2017 Apr 15;28(8):1054–65.

204. Friedberg F. Alternative splicing for members of human mosaic domain superfamilies. I. The CH and LIM domains containing group of proteins. Mol Biol Rep. 2008 Jun 16;36(5):1059–81.

205. Zhang Y, Zhang Y, Xu H. LIMCH1 suppress the growth of lung cancer by interacting with HUWE1 to sustain p53 stability. Gene. 2019 Sep 5;712:143963.

206. Martini N, Bains MS, Burt ME, Zakowski MF, McCormack P, Rusch VW, et al. Incidence of local recurrence and second primary tumors in resected stage I lung cancer. J Thorac Cardiovasc Surg. 1995 Jan;109(1):120–9.

207. Johnsson A, Olsson C, Nygren O, Nilsson M, Seiving B, Cavallin-Stahl E. Pharmacokinetics and tissue distribution of cisplatin in nude mice: platinum levels and cisplatin-DNA adducts. Cancer Chemother Pharmacol. 1995;37(1-2):23–31.

208. Marquet P, Lachatre G, Debord J, Eichler B, Bonnaud F, Nicot G. Pharmacokinetics of vinorelbine in man. Eur J Clin Pharmacol. 1992;42(5):545–7.

209. Goa KL, Faulds D. Vinorelbine. Drugs & Aging. 1994;5(3):200–34.

210. Yan Z, Jiang J, Li F, Yang W, Xie G, Zhou C, et al. Adenovirus-mediated LRIG1 expression enhances the chemosensitivity of bladder cancer cells to cisplatin. Oncol Rep. 2015 Apr;33(4):1791–8.

211. Zhou L, Li X, Zhou F, Jin Z, Chen D, Wang P, et al. Downregulation of leucine-rich repeats and immunoglobulin-like domains 1 by microRNA-20a modulates gastric cancer multidrug resistance. Cancer Sci. 2018 Apr;109(4):1044–54.

212. Wu X, Hedman H, Bergqvist M, Bergström S, Henriksson R, Gullbo J, et al. Expression of EGFR and LRIG proteins in oesophageal carcinoma with emphasis on patient survival and cellular chemosensitivity. Acta Oncol. 2012 Jan;51(1):69–76.